

Beyond the Iron Peak: r- and s-process Elemental Abundances in Stars with Planets

J. C. Bond¹, D. S. Lauretta¹, C. G. Tinney^{2,3}, R. P. Butler⁴, G. W. Marcy⁵, H. R. A. Jones⁶, B. D. Carter⁷, S. J. O'Toole³ & J. Bailey⁸

ABSTRACT

We present elemental abundances of 118 stars (28 of which are known extrasolar planetary host stars) observed as part of the Anglo-Australian Planet Search. Abundances of O, Mg, Cr, Y, Zr, Ba, Nd and Eu (along with previously published abundances for C and Si) are presented. This study is one of the first to specifically examine planetary host stars for the heavy elements produced by neutron capture reactions. We find that the host stars are chemically different to both the standard solar abundance and non-host stars in all elements studied, with enrichments over non-host stars ranging from 0.06 dex (for O) to 0.11 dex (for Cr and Y). Such abundance trends are in agreement with other previous studies of field stars and lead us to conclude that the chemical anomalies observed in planetary host stars are the result of normal galactic chemical evolution processes. Based on this observation, we conclude that the observed chemical traits of planetary host stars are primordial in origin, coming from the original nebula and not from a “pollution” process occurring during or after formation and that planet formation occurs naturally with the evolution of stellar material.

Subject headings: stars: abundances - stars: planetary systems - stars: chemical peculiar

¹Lunar & Planetary Laboratory, University of Arizona, 1629 E. University Blvd, Tucson, AZ 85721-0092

²Dept. of Astrophysics, University of NSW, NSW 2052, Australia

³Anglo-Australian Observatory, PO Box 296, Epping, NSW 1710, Australia

⁴Department of Terrestrial Magnetism, Carnegie Institution of Washington, 5241 Broad Branch Road NW, Washington, DC 20015-1305

⁵Department of Astronomy, University of California, Berkeley, CA 94720

⁶Centre for Astrophysics Research, University of Hertfordshire, College Lane, Hatfield AL10 9AB, England

⁷Faculty of Sciences, University of Southern Queensland, Toowoomba 4350, Australia

⁸Physics Department, Macquarie University, Sydney, NSW 2109, Australia

1. Introduction

Extrasolar planets are known to preferentially orbit metal-enhanced stars. Chemical analyses of known host stars have shown that they appear to be metal enriched compared to a sample of “average” F, G and K stars not known to harbour planets (Gonzalez 1997, 1998; Gonzalez & Vanture 1998; Gonzalez, Wallerstein & Saar 1999; Gonzalez & Laws 2000; Santos et al. 2000, 2001, 2004; Gonzalez et al. 2001; Smith et al. 2001; Reid 2002; Fischer & Valenti 2005; Bond et al. 2006). In addition to this global metal enrichment, individual elements have also been shown to exhibit similar trends, although not as statistically significant or with such large host and non-host differences (Gonzalez et al. 2001; Santos et al. 2000; Bodaghee et al. 2003; Fischer & Valenti 2005; Bond et al. 2006).

The vast majority of abundance studies completed so far have focussed on elements with atomic number (Z) ≤ 30 (i.e. those located before the iron stability peak). These elements are produced by a variety of processes (for example alpha particle addition, the CNO cycle and stellar burning reactions) in stellar interiors during main sequence evolution. Elements located beyond the iron peak, however, are produced via neutron-capture reactions, specifically the rapid (r-) and slow (s-) processes. Here rapid and slow refers to the speed of neutron capture with respect to the β -decay rate of the nuclei. In the r-process, neutron capture occurs before β -decay of the unstable nuclei can occur. Alternatively, in the s-process neutron capture occurs less frequently, thus allowing the nuclei to undergo β -decay before capturing another neutron and effectively allowing the nuclide to remain within the valley of β stability.

Due to the different neutron fluxes required for each process ($\sim 10^{23}$ neutrons $\text{cm}^{-2} \text{s}^{-1}$ for the r-process vs. $\sim 10^5$ neutrons $\text{cm}^{-2} \text{s}^{-1}$ for the s-process (Clayton 1968)), the r- and s-processes occur in different stellar environments. There is some debate as to exactly where the r-process occurs (see e.g. Qian 2004), but it is believed to primarily occur in type II supernova events. The s-process is thought to produce its heavier elements (such as Ba and Ce) in the interior of lower mass AGB stars and its lighter elements (such as Sr, Y and Zr) during the He-burning stages of stellar evolution for larger mass stars (Reddy et al. 2003). Due to these vastly different settings, the abundances of the heavy elements produced by these processes can provide information on the history of the material later incorporated into both the host star and planets themselves, as well as testing models of galactic chemical evolution (e.g. Fenner et al. 2006 and Lanfranchi et al. 2008). These elements have been part of several previous spectroscopic studies of stars without planets (e.g. Edvardsson et al 1993; Reddy et al. 2003; Allende Prieto et al. 2004; Bensby et al. 2005; Reddy et al. 2006), however only Ba (Huang et al. 2005) and Eu (Gonzalez & Laws 2007) have been specifically examined in a small number of known extrasolar planetary host stars.

Studies of stellar abundances have become critical to our understanding of planetary formation processes. However, in spite of significant advances in atmospheric models, stellar interiors and atomic line data in recent years, the measurement of stellar abundances is still an intricate process. In particular, choices made in the way an analysis is carried out can result in systematic abundance differences on sizes similar to the effects we would most like to understand in the stars themselves. Additionally, in many cases there is no consensus on the “correct” choice in these techniques.

To make headway in this field, therefore, it is essential to perform abundance studies in a manner immune to such systematic errors, by analysing both samples of interest, and control samples, in an identical manner. For the abundances of exoplanetary host stars, that means both host and non-host stars must be analysed in an identical manner. This is the primary goal of this current study.

We have derived abundances of five r- and s-process elements, in addition to three other lighter elements, for all the planet-hosting and non-planet-hosting stars in the Anglo-Australian Planet Search (AAPS) data set with viable template spectra, so that robust conclusions can be reached about the differences in their elemental abundances. The inclusion of these heavy elements begins to extend the spectroscopic studies of known host stars beyond the iron peak, thus continuing the search for additional chemical anomalies within these systems, while also providing an independent check of nucleosynthesis models and previously published abundances and trends for known host stars. The lighter elements selected for study (O, Mg and Cr) are included so as to complement the previous study of Bond et al. (2006) while also providing valuable information as to the cause of the metal-enrichment commonly seen in known host stars.

2. Data

2.1. Target Stars

In this study, we concentrate on the F- and G-type stars, observed at the 3.9m Anglo-Australian Telescope (AAT) since January 1998 as part of the AAPS program (Butler et al. 2001, 2002; Tinney et al. 2001, 2002, 2003, 2005, 2006; Jones et al. 2002, 2003, 2006; Carter et al. 2004; McCarthy et al. 2004; Jenkins et al. 2006; Wright et al. 2007; O’Toole et al. 2007). As at January 2007, 31 stars present within the AAPS sample were known to be planet hosts, of which 28 had spectra useful for the purposes of this study. Stars known to be young (age < 3 Gyr), active ($\log R'_{HK} > -4.5$) or with other stars within $5''$ are rejected from the AAPS search. For a more detailed description of the data and details of the criteria applied to the

AAPS target stars, the reader is referred to Butler et al. (1996) and Tinney et al. (2005). Of the 28 host stars considered here, 26 have had some common elemental abundances previously determined by other authors.

2.2. Spectroscopic Analysis

The method utilised in this study closely follows that outlined in Bond et al. (2006) who studied Fe, C, Na, Al, Si, Ca, Ti and Ni. Spectra encompassing the entire visible spectrum from 4820 to 8420Å with a signal-to-noise ratio (S/N) between 200 and 300 per spectral pixel at resolution $\lambda/\Delta\lambda \approx 80000$ were obtained via the University College London Echelle Spectrograph (UCLES) using the 31.6 line/mm echelle grating as part of the AAPS program. The raw data were reduced and processed so as to produce a one-dimensional spectra, suitable for spectral analysis.

We do differ slightly from Bond et al. (2006) in the method used to determine the equivalent widths of absorption lines. In Bond et al. (2006), we obtained equivalent width estimates via direct integration over the line. In this study we follow the method of other similar studies (eg. Santos et al. 2000; Gonzalez et al. 2001; Santos et al. 2001) and make Gaussian line fits to the spectra using the IRAF task `splot` in the package `noao.onedspec` (due to difficulties in automating the previous script). This slight difference in methodology does not produce any significant difference in the final abundances obtained.

Five heavy elements were analysed for the first time as part of this study and they were primarily selected based on their process of production. Y, Zr and Ba are all produced primarily by the s-process while Eu is primarily produced by the r-process and Nd is an almost even mix between the two based on Solar System abundances (Arlandini et al. 1999; Simmerer et al. 2004). The line list utilised in this study is shown in Table 1 and is derived from Gilli et al. (2006) (for Mg and Cr), Reddy et al. (2003) (for Y, Zr, Ba, Eu and Nd) and Den Hartog et al. (2003) (for Nd). Additional Ba lines have been used in other studies, but were neglected here as they gave consistently lower abundances by approximately 0.60 dex. While the use of more lines in determining an abundance should produce a more robust value, we could not determine the cause of this offset and elected instead to use the single stronger line at 6496.91Å as this line produced a Ba abundance close to the reported solar value for a solar spectrum. Atomic parameters for each line were obtained from the NIST Atomic Spectra Database, Version 3.0 (for O, Mg and Cr), Pitts & Newsom (1986) and Hannaford et al. (1982) (for Y), Reddy et al. (2003) (for Ba), Den Hartog et al. (2003) (for

Nd) and the Kurucz atomic line database¹ (for Zr and Eu). All of the atomic parameters applied here have also been utilised in previous studies and produce solar elemental abundances well within errors of those published elsewhere, when applied to a solar spectrum, thus giving us confidence in applying them here.

Elemental abundances were obtained via standard local thermodynamic equilibrium analysis, as has been done by previous studies (see Santos et al. 2000; Gonzalez et al. 2001; Santos et al. 2001; Bond et al. 2006). A revised version of Sneden’s (1973) MOOG abundance code entitled `width6` (Ryan 2005) was once again used in conjunction with a grid of Kurucz (1993) ATLAS9 atmospheres² to obtain the final elemental abundances. As all of the non-host, and all but 7 of the host stars, had been the subject of an earlier study (Bond et al. 2006), previously published stellar atmospheric parameters were used. For those stars without previously determined values, we followed the same method as used in Bond et al. (2006) to obtain the values and refer the reader to the paper for more details. As the OI triplet lines are known to suffer from non-LTE effects, the corrections of Takeda (2003) for $\xi_t=1\text{km/s}$ and $\log g=4.0\text{ cm/s}^2$ were applied to obtain our final O abundances. When applied to a solar spectrum, this method produced abundances in agreement with those of Asplund et al. (2005).

3. Results

The stellar elemental abundances are shown in Table 2 (in the standard astronomical logarithmic form) and Table 3 (in the more cosmochemically useful form with abundances normalized to 10^6 Si atoms). The notation of – for an abundance indicates that a value could not be obtained from the spectrum due to noise. Additionally, for ease of comparison in Section 5.1, C and Si stellar elemental abundances, along with the normalized C abundances, for all target stars are presented in Table 4. The C and Si abundances were previously published in Bond et al. (2006).

Other authors have previously determined abundance values for several of the elements also studied here with many of these abundances differing from our values. Differences between our present study and that of others is not a significant issue for the primary thrust of this paper, which is to compare host and non-host stellar abundances which have been measured in an identical fashion. However, in the interests of completeness we note that Mg

¹<http://www.pmp.uni-hannover.de/cgi-bin/ssi/test/kurucz/sekur.html>

²<http://kurucz.harvard.edu> or <http://www.stsci.edu/hst/observatory/cdbs/k93models.html>

abundances were determined for 29 common stars (20 hosts) by Berião et al. (2005), Cr in 28 stars (20 hosts) and Mg in 29 stars (20 hosts) by Gilli et al. (2006), Cr in 25 stars (16 hosts) by Bodaghee et al. (2003), O in 8 stars (4 hosts) by Ecuivillon et al. (2006), O and Eu in 4 host stars, Cr and Mg in 1 host star by Gonzalez & Laws (2007) and O in 1 host star by Santos et al. (2000). The mean differences between our values and those previously published are shown in Table 5 (for those samples having more than one common star) with the difference being defined as the abundance from this study minus the published abundance. Generally, our results can be seen to be in agreement with those previously published for Cr and O with a significantly larger mean difference occurring for Mg and a large deviation occurring for Eu. The differences between our abundances and those previously published are believed to be due to the use of a smaller number of lines in determining the abundance (for Mg), the use of different methods (for O and Eu), the use of different atomic parameters (for Eu) and the use of different non-LTE corrections (for O).

4. Host Star Enrichment

4.1. Enrichment over Solar

The mean and median abundances, standard deviation and the difference between the host and non-host stars for all of our target stars can be seen in Table 6 for each element. The quoted uncertainties are the standard error in the mean, and the median uncertainty from the algorithm of Kendall, Stuart & Ord (1987)³. The mean values of this study for the known host stars are all consistent to within the 1σ value of those listed by Berião et al. (2005) and Gilli et al. (2006). The data show that in general known extrasolar planetary host stars differ only slightly from the mean solar abundance patterns with all of the median abundances being well within 1σ of the solar abundance - as concluded by previous studies (eg. Ecuivillon et al. 2004; Bodaghee et al. 2003). This is reassuring as the Sun is itself obviously a planetary host star with abundances enhanced over those of most other stars in the solar neighbourhood (based on the abundances of Asplund et al. 2005). In many respects, therefore, the Sun is *not* a typical field star, based on its abundances and its multiple planetary companions. The largest enrichment over solar is seen in Nd and Zr, with Cr showing a smaller enrichment and Mg showing minimal enrichment. Eu showed the largest depletion relative to solar values, with Y and Ba also showing mild to moderate depletions. Only O produced a mean abundance equal to the Solar abundance.

³For a distribution with N values, the error in the median is the range in values on either side of the median which contains $(\sqrt{N})/2$ values

Similarly, the non-host stars can also be seen to be depleted when compared to solar abundances for almost all of the elements studied, with the largest depletion being -0.16 for Y and Eu. It is also worth noting that three of the five heavy elements examined show a mean depletion relative to solar for both the host and non-host stars. Of these three, two are produced by the s-process (Y & Ba) with the remaining element (Eu) produced by the r-process.

4.2. Enrichment over Non-Host Stars

A more powerful comparison is obtained by comparing our host and non-host populations to each other. On doing so, it can be clearly seen that host stars are systematically enriched over non-host stars in all elements studied. The enrichment ranges in size from 0.06 (for O) to 0.11 for (for Cr and Y) (see Table 6).

This difference between the host and non-host populations can also be seen in the results of the Kolmogorov-Smirnov (K-S) statistical test. Designed to test whether two populations were drawn from the same parent sample, the K-S test showed a significant difference between the host and non-host samples with probabilities of a different parent sample ranging from 91.2% for O to 99.99% for Y (see Table 6). This supports our claim that host star elemental abundances are significantly different to those of non-host stars and furthermore that host stars are enriched over non-host stars for all elements studied.

5. Elemental Trends

Plots of our results are shown in Figures 1 and 2 - in Figure 1 we present $[X/H]$ versus $[Fe/H]$ as more commonly used in previous studies of planet host star abundances, while in Figure 2 we present $[X/Fe]$ versus $[Fe/H]$ as usually analysed in cosmochemical studies. Two significant outliers can be seen - one host and one non-host sitting below the general trend for O, Cr and Mg. These stars are HD142415 ($[Fe/H]=0.02$, host) and HD199288 ($[Fe/H]=0.04$, non-host). These stars can be seen to be depleted (compared to solar abundances) in the majority of elements studied here except for Fe, suggesting that they have formed from Fe-rich precursor material based on the assumption that it is easier to enrich one element than it is to deplete seven elements. The fact that HD142415 is also mildly enriched in both Ba and Y (with no Zr abundance available) could also possibly indicate that the material had been processed through an s-process environment, either an AGB star or the He-burning stage of a larger mass star.

Fe and Fe precursors: The $[X/H]$ trends in Figure 1 are in agreement with the understanding we currently have about the nucleosynthetic origin of the elements. All of the elements located before the Fe peak (here O, Mg and Cr) increase linearly with increasing $[Fe/H]$ with Pearson product-moment correlation coefficients (r) above 0.70 for both host and non-host stars. This can be easily understood as the stellar evolutionary processes that serve to increase the amount of Fe present in later generations of stars also produce the pre-iron peak elements in various amounts. Thus as the stellar Fe content increases, so too would the amount of pre-iron peak elements (neglecting any unusual mixing or other nebula interactions).

s-process: The r- and s-process elements, however, are less certain. All three s-process elements (Y, Zr and Ba) still display to varying degrees the same trend of increasing abundance with increasing $[Fe/H]$ as the pre-iron peak elements. One possible explanation for this observed trend is that the increase in s-process elemental abundances is due to the increase in the number of seed nuclei (e.g. Fe atoms) available. Due to the nature of the s-process, it is reliant on the sufficient availability of seed nuclei to be able to proceed. Thus as the metallicity increases, so too does the abundance of s-process species.

r-process: Unlike the s-process elements, the r-process element (Eu) and the mixed source element (Nd) do not display a strong correlation with increasing $[Fe/H]$. Observations of metal poor stars have shown that the abundances of s-process elements such as Y and Ba decrease faster with metallicity than the abundances of r-process elements such as Eu (Spite & Spite 1978). This has been attributed to a lack of appropriate seed nuclei inhibiting the s-process significantly more than the r-process. We are alternatively extending this into the metal-rich regime to conclude that the r-process is not as reliant on the presence of elements such as Fe, thus explaining its lack of a strong dependance upon metallicity.

From Figure 2, it can be seen that the overall $[X/Fe]$ trends visible here are in good agreement with those identified by Bodaghee et al. (2003) and Gilli et al. (2006) (which are discussed in more detail below). They can also be seen as extensions into the high metallicity region of those trends identified by Reddy et al. (2006).

5.1. Lighter Element Trends

In addition to examining the nature of the general trend of increasing elemental abundances with increasing metallicity, we can also make some basic determinations about the nature of the various nucleosynthesis processes occurring within the precursors to these systems by considering the more subtle, second order trends present within the data.

O: Based on our data, [O/Fe] displays a weakly correlated decreasing trend with increasing [Fe/H] for both the host stars (slope= -0.16 , $r=-0.22$) and non-host stars (slope= -0.24 , $r=-0.32$). Previous studies have hinted at the possibility of a plateau starting at [Fe/H] ~ 0 (Reddy et al. 2003, Reddy et al. 2006). However, the overlap between our sample and those previously published is not large enough to allow us to undertake any meaningful comparison. It is also worth noting that while the solar C/O ratio is 0.54 (Asplund et al. 2005), using the [C/H] values previously published by Bond et al. (2006) (see Table 4), the C/O values of the host stars studied here range from 0.40 to 0.89. This variation has the potential to greatly impact the C chemistry of the proto-stellar disc and thus also any terrestrial planets forming in the system. Further studies into this subject are currently underway (see Bond et al. 2008).

Mg: [Mg/Fe] can be seen to display a weakly correlated trend of decreasing with increasing [Fe/H] values producing r values of -0.32 (host stars) and -0.44 (non-host stars). The distribution observed for Mg is in good agreement (for the [Fe/H] regions in common) with those of previous studies who observed a decrease in [Mg/Fe] with increasing [Fe/H] up to [Fe/H] ~ -0.10 before both distributions plateaued (Berião et al. 2005; Gilli et al. 2006; Reddy et al. 2006).

Also of interest is the Mg/Si ratio of our target stars as it has the potential to greatly affect the chemical evolution of any terrestrial planets forming in the system. A high Mg/Si ratio will result in all of the available Si forming olivine ($(\text{Fe,Mg})_2\text{SiO}_4$) with excess Mg still being available, while a low Mg/Si ratio will result in all of the available Mg forming enstatite (MgSiO_3) with excess Si forming SiO_2 . Utilising the Si abundances previously published in Bond et al. (2006) (see Table 4), the host stars of this study were found to have Mg/Si ratios ranging from 0.46 to 1.26, resulting in potentially large variations in the nature of any terrestrial planets forming in these systems. A separate study examining this issue is currently underway (see Bond et al. 2008).

Fe Group (Cr): From Figure 2, it can be seen that (with the exception of one outlier) [Cr/Fe] displays no significant trend, remaining largely unchanged over all of the [Fe/H] values considered here. This is in good agreement with Reddy et al. (2003); Bensby et al. (2005) and Gilli et al. (2006). The lack of a statistically significant trend with [Fe/H] is confirmed by the low r value of -0.04 for hosts and 0.00 for non-hosts.

5.2. Heavy Element Trends

From Figure 2, it can be seen that all of the heavy elements display varying degrees of a weakly negative to non-existent correlation with $[\text{Fe}/\text{H}]$. The r values produced range from -0.22 (Y and Ba) to -0.56 (Nd) indicating that the correlation is not strong.

These trends are in agreement with Allende Prieto et al. (2004) and Bensby et al. (2005) over the range of metallicity values in common with this study. We do differ slightly from some previous studies in that we observed a stronger decrease in $[\text{Y}/\text{Fe}]$ with increasing $[\text{Fe}/\text{H}]$ than was observed by Bensby et al. (2005) and disagree with previous studies who observed no significant trend with $[\text{Fe}/\text{H}]$ for both $[\text{Ba}/\text{Fe}]$ and $[\text{Nd}/\text{Fe}]$ (Reddy et al. 2003). We do observe trends in both of these samples and the difference is attributed to the fact that we are examining a different metallicity region to that of Reddy et al. (2003). Our population is largely concentrated in the region of $[\text{Fe}/\text{H}] > 0$, while the sample of Reddy et al. (2003) almost exclusively has values of $[\text{Fe}/\text{H}] < 0$. However, it is worth restating that the general trends in the neutron capture elements identified here are the same as those previously identified for other solar-type stars. This implies that the host stars examined in this paper follow the same trends as other field stars but with a bias towards the high metallicity region. Additionally, the high degree of scatter observed in these samples is also in agreement with previous studies.

Also of interest is the ratio of the heavy to light s-process elements as each are thought to be produced in slightly different stellar settings. The abundance of the heavy s-process element Ba to the light s-process elements Y and Zr is shown in Figure 3 as $[\text{heavy}/\text{light}]$ where:

$$[\text{heavy}/\text{light}] = [\text{Ba}/\text{H}] - \frac{[\text{Y}/\text{H}] + [\text{Zr}/\text{H}]}{2}$$

From Figure 3, it can be clearly seen that there is no dependence on metallicity, with values scattering around the solar value (0.0 by definition). This is in agreement with Reddy et al. (2003). Thus we support their conclusion that the neutron exposure in AGB stars is independent of the metallicity of the star itself, assuming (as Reddy et al. 2003 did) that AGB stars are the primary source of both the heavy and the light s-process elements.

5.3. Correlation with Planetary Parameters

Figure 4 shows plots of $[X/H]$ against planetary parameters ($M\sin i$, semi-major axis a , eccentricity and planetary period) for the 5 heavy elements considered in this study. HD164427 was omitted as its companion is believed to be a brown dwarf, not a gas giant. As can be seen visually and by the low r values (all ≤ 0.48 with most < 0.15), no statistically significant correlations exist between these abundances and any of the orbital parameters. This agrees with previous studies of other elements (eg. Reid 2002; Santos et al. 2003; Fischer & Valenti 2005).

5.4. Correlation with Stellar Parameters

It is well known that the stellar atmospheric parameters (specifically T_{eff} and $\log g$) have the potential to drastically alter photospherically determined stellar abundances. As such, we examined the abundances presented here and as both samples produced r^2 correlation coefficients less than 0.5, we concluded that there is no statistically significant trends present with either the stellar T_{eff} or $\log g$ values.

6. Discussion

The host stars studied here do not significantly deviate from previously established galactic chemical evolution trends. Instead, they can be regarded as being extensions of many of those trends into metallicities above solar. This lack of deviation from previously known trends strongly suggests that while they are more metal enriched than other stars not known to host planets, the host stars themselves have not systematically undergone any extraordinary chemical processing during their growth and evolution (in agreement with Robinson et al. 2006). The conclusion that planetary hosts stars are essentially “normal” may indeed suggest that planetary formation is a normal result of the star formation process. Of course, this does not exclude planet formation at lower metallicity values (as planets have been detected orbiting stars with metallicities significantly below solar) nor does it guarantee planet formation at high metallicity values.

There are two primary hypotheses that have been offered to explain the observed high metallicity trend. The first is the “pollution” model which posits metal-rich material being added to the photosphere as a consequence of planetary formation (Laughlin 2000; Gonzalez et al. 2001; Murray & Chaboyer 2002). The second explanation is commonly referred to as the primordial model and it suggests that the gas cloud from which these systems

formed was metal enriched, resulting in the star itself being enriched in the same elements (Santos et al. 2001). Our conclusion that these host stars exhibit normal chemical evolution trends and that they are simply the metal-rich members of field star population lends support to the primordial model. One would expect that pollution of the stellar photosphere would produce deviations from the galactic evolutionary trends. To date no such trends have been observed. Additionally, we also observe that the abundances of the more volatile elements (such as O) increase with increasing metallicity for both the host and non-host stars. This would not be the case in the pollution model as it is likely that only the more refractory elements (such as Fe and Ni) would remain in the solid form as they migrated towards the star (and thus be deposited in the stellar photosphere) while the more volatile elements would be evaporated before they could be incorporated into the stellar photosphere. As such, we would expect to see enrichment only in the refractory elements and not the volatile elements if the pollution model is accurate. Furthermore, the fact that we observe no trends with metallicity in the orbital parameters of the remaining planets is difficult for the pollution model to explain. It is hard to imagine a situation whereby almost *all* planetary host stars accreted a significant amount of material during planetary formation without affecting the orbital parameters of the remaining planets. For these reasons, we agree with previous studies (such as Santos et al. 2001, 2003, 2004, 2005 and Fischer & Valenti 2005) and support the primordial model for explaining the metal enrichment in planetary host stars.

The abundances reported here also impact on terrestrial planet formation and evolution within these systems. Those with low Mg/Si ratios will have terrestrial planets dominated by enstatite (with a small amount of Mg-rich olivine also present) with other Si-based species also available (a composition similar to the Earth’s crust), while those with high Mg/Si ratios will have olivine-dominated planets with other Mg-rich species also present (a composition similar to the Earth’s mantle). Similarly, a high C/O ratio will result in planets with greatly increased C contents due to solid C being incorporated into the planet itself. While the detailed consequences of these examples have not yet been fully examined, it is conceivable that any terrestrial planets forming in these systems could differ from currently known terrestrial planets in terms of their rheology (thus possibly affecting the tectonics of such a planet) and the nature of volcanic activity, based on the varying silica contents of the magma. The full implications of such a chemical composition for the evolution of the terrestrial planets themselves is the subject of ongoing research.

7. Summary

In this paper, we have presented elemental abundances for 8 elements, including 5 heavy elements produced by the r- and s-processes, in 28 planetary host stars and 90 non-host stars from the AAPS. We conclude that while the elemental abundances of the planetary host stars are only slightly different from solar values, the host stars are enriched over the non-hosts stars in all elements studied with the mean difference varying from 0.06 dex to 0.11 dex.

Additionally, we also considered the trends of the abundances (both $[X/H]$ and $[X/Fe]$) with $[Fe/H]$ and found these to be largely in keeping with known galactic chemical evolution trends. This implies that these systems have followed normal evolutionary pathways and are not significantly or unusually altered. This leads us to conclude that not only are the abundance trends we are observing primordial in origin and represent the initial composition of the gas nebula that produced the star and its planets but that planetary formation may also be a natural companion to the evolution of stellar material.

We would like to thank Sean Ryan for his assistance with this study by providing the stellar atmosphere and abundance code, along with incredibly patient help. We would also like to thank the anonymous reviewer for their useful suggestions and advice. The Anglo-Australian Planet Search team would like to acknowledge support by the partners of the Anglo-Australian Telescope Agreement (CGT and HRAJ); NASA grant NAG5-8299, NSF grant AST 95-20443 (GWM), NSF grant AST 99-88087 (RPB), PPARC grant PP/C000552/1 (HRAJ, CGT, SJO) and ARC grant DP0774000 (CGT). This research has made use of the SIMBAD database, operated at CDS, Strasbourg, France, and the NASA Astrophysics Data System.

REFERENCES

- Allende Prieto, C., Barklem, P. S., Lambert, D. L. & Cunha, K., 2004, *A&A*, 420, 183
- Arlandini, C., Käppeler, F., Wisshak, K., Gallino, R., Lugaro, M., Busso, M. & Straniero, O., 1999, *ApJ*, 525, 886
- Asplund, M., Grevesse, N. & Sauval, A. J., 2005, *ASPC*, 336, 25A
- Bensby, T., Feltzing, S. & Lundström, I., 2003, *A&A*, 410, 527
- Bensby, T., Feltzing, S., Lundström, I. & Ilyin, I., 2005, *A&A*, 433, 185

- Bond, J.C., Tinney, C. G., Butler, P. R., Jones, H. R. A., Marcy, G. W., Penny, Alan J. & Carter, B. D., 2006, MNRAS, 370, 163
- Bond, J.C., Laretta, D. S. & O'Brien, D. P., 2008, LPSC XXXIX, Abstract 1438
- Berião, P., Santos, N. C., Isralian, G. & Mayor, M. 2005, A & A, 438, 251
- Bodaghee, A., Santos, N. C., Isralian, G. & Mayor, M. 2003, A & A, 404, 715
- Butler, P. R., Marcy, G. W., Williams, E., McCarthy, C. & Vogt, S. S., 1996, PASP, 108, 500
- Butler, P. R., Tinney, C. G., Marcy, Geoffrey W., Jones, Hugh R. A., Penny, Alan J. & Apps, Kevin, 2001, ApJ, 555, 410
- Butler, P. R., et al., 2002, ApJ, 578, 565
- Carter, B. D., Butler, R. P., Tinney, C. G., Jones, H. R. A., Marcy, G. W., McCarthy, C., Fischer, D. A. & Penny, A. J., 2003, ApJ, 593, L43
- Clayton, D. D., 1968, Principles of Stellar Evolution and Nucleosynthesis, 1st edn. McGraw-Hill Book Company, New York, pp. 557.
- Den Hartog, E. A., Lawler, J. E., Sneden, C. & Cowan, J. J., 2003, ApJ Supp. Ser., 148, 543
- Ecuivillon, A., Isralian, G., Santos, N. C., Mayor, M., Villar, V. & Binhain, G. 2004, A & A, 426, 619
- Ecuivillon, A., Isralian, G., Santos, N. C., Shchukina, N. G., Mayor, M. & Rebolo, R. 2006, A & A, 445, 633
- Edvardsson, B., Andersen, J., Gustafsson, B., Lambert, D. L., Nissen, P. E. & Tomkin, J., 1993, A & A, 275, 101
- Fenner, Y., Gibson, B. K., Gallino, R. & Lugaro, M., 2006, ApJ, 646, 184
- Fischer, D. A. & Valenti, J., 2005, ApJ, 662, 1102
- Gilli, G., Israelian, G., Ecuivillon, A., Santos, N. C. & Mayor, M., 2006, A&A, 449, 723
- Gonzalez, G., 1997, MNRAS, 285, 403
- Gonzalez, G., 1998, A & A, 334, 221
- Gonzalez, G. & Laws, C., 2000, AJ, 119, 390

- Gonzalez, G. & Laws, C., 2007, MNRAS, 378, 1141, 1152
- Gonzalez, G., Laws, C., Tyagi, S. & Reddy, B. E., 2001, AJ, 121, 432
- Gonzalez, G. & Vanture, A. D., 1998, A & A, 339, L29
- Gonzalez, G., Wallerstein, G. & Saar, S. H., 1999, ApJ, 511, L111
- Hannaford, P., Lowe, R. M., Grevesse, N., Biéumont, E. & Whaling, W., 1982, ApJ, 261, 736
- Huang, C., Zhao, G., Zhang, H. W. & Chen, Y. Q., 2005, MNRAS, 363, 71
- Jenkins, J. S., Jones, H. R. A., Tinney, C. G., Butler, R. P., McCarthy, C., Marcy, G. W., Pinfield, D. J., Carter, B. D. & Penny, A. J., 2006, MNRAS, 372, 163
- Jones, H. R. A., Butler, R. P., Tinney, C. G., Marcy, G. W., Penny, A. J., McCarthy, C. & Carter, B. D., 2002, MNRAS, 333, 871
- Jones, H. R. A., Butler, R. P., Marcy, G. W., Tinney, C. G., Penny, A. J., McCarthy, C., Carter, B. D. & Bailey, J., 2006, MNRAS, 369, 249
- Jones, H. R. A., Butler, R. P., Tinney, C. G., Marcy, G. W., Carter, B. D., Penny, A. J., McCarthy, C. & Carter, B. D., 2002, MNRAS, 333, 871
- Kendall, M. G., Stuart, A. & Ord, J. K., 1987, Kendall's Advanced Theory of Statistics, 5th edn. Oxford University Press, New York
- Kurucz, R. L., 1993, CD-ROMSs, ATLAS9 A Stellar Atmospheres Program and 2 km.s⁻¹ Grid (Cambridge: Smithsonian Astrophys. Obs.)
- Lanfranchi, G. A., Matteucci, F. & Cescutti, G., 2008, A&A, 431, 635
- Laughlin, G., 2000, ApJ, 545, 1064
- Marcy, G.W. & Butler, R.P. 1996, ApJ, 464, L147
- McCarthy, C., et al., 2004, ApJ, 617, 575
- Murray, N. & Chaboyer, B., 2002, ApJ, 566, 442
- O'Toole, S. J., Butler, R. P., Tinney, C. G., Jones, H. R. A., Marcy, G. W., Carter, B. D., McCarthy, C., Bailey, J., Penny, A. P., Apps, A. & Fischer, D., 2007, ApJ, 660, 1636
- Pits, R. E. & Newsom, G. H., 1986, J. Quant. Spec. Rad. Transfer., 35, 383

- Qian, Y.-Z., 2004, *Prog. Part. Nuc. Phys.*, 150, 153
- Reddy, B. E., Tomkin, J., Lambert, D. L. & Allende Prieto, C., 2003, *MNRAS*, 340, 304
- Reddy, B. E., Lambert, D. L. & Allende Prieto, C., 2006, *MNRAS*, 367, 1329
- Reid, I. N., 2002, *PASP*, 114, 306
- Robinson, S. E., Laughlin, G., Bodenheimer, P. & Fischer, D., 2006, *ApJ*, 643, 484
- Ryan, S.G., 2005, Personal Communication
- Santos, N. C., Israelian, G. & Mayor, M., 2000, *A & A*, 363, 228
- Santos, N. C., Israelian, G. & Mayor, M., 2001, *A & A*, 373, 1019
- Santos, N. C., Israelian, G., Mayor, M., Rebolo, R. & Udry, S., 2003, *A & A*, 398, 363
- Santos, N. C., Israelian, G. & Mayor, M., 2004, *A & A*, 415, 1153
- Santos, N. C., Israelian, G., Mayor, M., Bento, J. P., Almeida, P. C., Sousa, S. G. & Ecuillon, A. 2005, *A & A*, 437, 1127
- Simmerer, J., Sneden, C., Cowan, J. J., Collier, J., Woolf, V. M., & Lawler, J. E., 2004, *ApJ*, 617, 1091
- Sneden, C., 1973, PhD Thesis, University of Texas
- Strömgen, B., 1966, *ARA&A*, 4, 433
- Smith, V., Cunha, K. & Lazzaro, D., 2001, *AJ*, 121, 3207
- Spite, M. & Spite, F., 1978, *A&A*, 67, 23
- Takeda, Y., 2003, *A&A*, 4402, 343
- Tinney, C. G., Butler, R. P., Marcy, G. W., Jones, H. R. A., Penny, A. J., Vogt, S. S., Apps, K. & Henry, G. W., 2001, *ApJ*, 551, 507
- Tinney, C. G., Butler, R. P., Marcy, G. W., Jones, H. R. A., Penny, A. J., McCarthy, C. & Carter, B. D., 2002, *ApJ*, 571, 528
- Tinney, C. G., Butler, R. P., Marcy, G. W., Jones, H. R. A., Penny, A. J., McCarthy, C., Carter, B. D. & Bond, J., 2003, *ApJ*, 587, 423

- Tinney, C. G., Butler, R. P., Marcy, G. W., Jones, H. R. A., Penny, A. J., McCarthy, C., Carter, B. D. & Fischer, D. A., 2005, *ApJ*, 623, 1171
- Tinney, C. G., Butler, R. P., Marcy, G. W., Jones, H. R. A., Penny, A. J., Laughlin, G., Carter, B. D., Bailey, J. A. & O’Toole, S., 2006, *ApJ*, 647, 594
- Valenti, J. & Fischer, D. A., 2005, *ApJ Supp. Ser.*, 159, 141
- Wright, J. T., Marcy, G. W., Fischer, D. A., Butler, R. P., Vogt, S. S., Tinney, C. G., Jones, H. R. A., Carter, B. D., Johnson, J. A., McCarthy, C. & Apps, K., 2007, *ApJ*, 657, 533

Table 1. Line list used for chemical abundance analysis

λ (Å)	Log gf	χ_l (eV)	λ (Å)	Log gf	χ_l (eV)
Mg I:			Y II:		
5711.09	-1.71	4.35	4854.87	-0.01	0.99
6318.72	-1.99	5.11	4900.12	-0.09	1.03
Cr I:			5087.43	-0.17	1.08
5304.18	-0.69	3.46	5200.42	-0.49	0.99
5312.87	-0.56	3.45	5402.78	-0.63	1.84
5318.81	-0.69	3.44	Zr II:		
5783.09	-0.50	3.32	5112.28	-0.59	1.66
5783.89	-0.29	3.32	Eu II:		
O I:			6645.13	0.20	1.38
7771.94	0.37	9.15	Nd II:		
7774.17	0.22	9.15	4914.18	-0.70	0.38
7775.39	0.002	9.15	5234.19	-0.51	0.55
Ba II:					
6496.91	-0.41	0.60			

Table 2. Stellar Abundances for all Target Stars. A – indicates that a value could not be obtained from the spectrum.

HD	[O/H]	[Cr/H]	[Mg/H]	[Ba/H]	[Y/H]	[Zr/H]	[Eu/H]	[Nd/H]
Host Stars:								
2039	0.09 ± 0.04	0.25 ± 0.07	0.15 ± 0.07	0.14 ± 0.03	0.14 ± 0.09	0.06 ± 0.03	0.00 ± 0.02	0.23 ± 0.25
4308	-0.13 ± 0.02	-0.27 ± 0.02	-0.22 ± 0.09	-0.44 ± 0.02	-0.44 ± 0.08	-0.18 ± 0.03	-0.06 ± 0.01	-0.17 ± 0.16
10647	-0.14 ± 0.02	-0.14 ± 0.06	-0.15 ± 0.06	0.07 ± 0.03	-0.13 ± 0.12	-0.02 ± 0.04	-0.30 ± 0.01	-0.28 ± 0.20
13445	-0.22 ± 0.03	-0.18 ± 0.03	-0.27 ± 0.09	-0.48 ± 0.08	-0.35 ± 0.10	–	-0.43 ± 0.06	-0.06 ± 0.03
17051	0.00 ± 0.01	0.08 ± 0.06	-0.13 ± 0.01	0.18 ± 0.08	0.00 ± 0.12	0.15 ± 0.04	-0.10 ± 0.03	0.07 ± 0.10
23079	-0.24 ± 0.02	-0.16 ± 0.05	-0.33 ± 0.01	-0.22 ± 0.03	-0.19 ± 0.10	-0.05 ± 0.09	-0.18 ± 0.04	-0.05 ± 0.10
20782	-0.46 ± 0.04	0.12 ± 0.05	0.02 ± 0.07	–	-0.32 ± 0.08	-0.35 ± 0.05	-0.32 ± 0.06	-0.21 ± 0.05
30177	0.30 ± 0.06	0.30 ± 0.08	0.07 ± 0.02	-0.11 ± 0.03	0.03 ± 0.11	-0.04 ± 0.05	–	0.23 ± 0.04
39091	–	0.15 ± 0.05	0.10 ± 0.03	–	–	-0.04 ± 0.03	-0.11 ± 0.04	-0.04 ± 0.01
70642	0.08 ± 0.02	0.21 ± 0.05	0.09 ± 0.07	0.00 ± 0.03	0.11 ± 0.07	0.24 ± 0.04	-0.05 ± 0.02	–
73526	0.08 ± 0.07	0.12 ± 0.05	0.07 ± 0.09	0.05 ± 0.02	-0.08 ± 0.13	0.23 ± 0.05	0.22 ± 0.06	0.11 ± 0.04
75289	0.01 ± 0.02	0.17 ± 0.04	0.00 ± 0.03	0.07 ± 0.10	0.02 ± 0.12	0.29 ± 0.04	0.04 ± 0.06	0.31 ± 0.05
83443	0.27 ± 0.07	0.29 ± 0.06	0.16 ± 0.06	-0.16 ± 0.02	0.06 ± 0.06	-0.05 ± 0.04	-0.08 ± 0.03	0.05 ± 0.04
102117	0.13 ± 0.04	0.22 ± 0.05	0.07 ± 0.08	0.11 ± 0.10	0.00 ± 0.08	0.23 ± 0.03	–	0.15 ± 0.05
108147	-0.07 ± 0.02	0.05 ± 0.05	-0.07 ± 0.02	0.04 ± 0.03	-0.03 ± 0.11	-0.07 ± 0.04	0.00 ± 0.02	-0.03 ± 0.10
117618	-0.09 ± 0.02	-0.07 ± 0.05	-0.06 ± 0.08	0.09 ± 0.11	-0.11 ± 0.10	0.01 ± 0.03	-0.07 ± 0.01	0.11 ± 0.04
134987	0.19 ± 0.04	0.30 ± 0.06	0.22 ± 0.09	0.31 ± 0.03	0.18 ± 0.08	0.21 ± 0.01	0.00 ± 0.03	0.27 ± 0.04
142415	-0.21 ± 0.01	-0.21 ± 0.05	-0.29 ± 0.01	0.11 ± 0.04	0.01 ± 0.10	–	-0.23 ± 0.03	0.11 ± 0.02
154857	-0.15 ± 0.03	-0.20 ± 0.04	-0.20 ± 0.03	-0.11 ± 0.09	-0.29 ± 0.08	-0.08 ± 0.04	-0.27 ± 0.07	-0.01 ± 0.02
160691	0.15 ± 0.02	0.20 ± 0.06	0.14 ± 0.10	0.01 ± 0.05	0.00 ± 0.08	0.20 ± 0.04	-0.16 ± 0.08	0.18 ± 0.02
164427	-0.02 ± 0.01	0.07 ± 0.03	-0.07 ± 0.01	-0.15 ± 0.03	-0.17 ± 0.10	-0.10 ± 0.05	-0.14 ± 0.04	0.12 ± 0.06
179949	0.03 ± 0.05	0.14 ± 0.04	0.04 ± 0.01	-0.23 ± 0.03	0.16 ± 0.07	0.28 ± 0.08	-0.05 ± 0.04	0.13 ± 0.10
187085	-0.05 ± 0.02	-0.01 ± 0.05	-0.14 ± 0.01	0.05 ± 0.07	-0.06 ± 0.15	0.08 ± 0.02	-0.32 ± 0.07	-0.02 ± 0.11
196050	0.17 ± 0.05	0.20 ± 0.06	0.19 ± 0.01	0.09 ± 0.04	0.09 ± 0.10	0.19 ± 0.05	-0.12 ± 0.04	0.02 ± 0.06
208487	-0.09 ± 0.01	0.02 ± 0.05	-0.10 ± 0.02	-0.06 ± 0.05	-0.06 ± 0.11	0.03 ± 0.03	-0.14 ± 0.07	-0.01 ± 0.04
213240	0.00 ± 0.02	0.09 ± 0.04	-0.04 ± 0.04	0.07 ± 0.02	-0.01 ± 0.12	0.09 ± 0.03	0.14 ± 0.07	0.23 ± 0.05
216435	0.21 ± 0.02	0.24 ± 0.04	0.18 ± 0.05	0.26 ± 0.09	0.19 ± 0.14	0.29 ± 0.05	0.00 ± 0.01	0.09 ± 0.15
216437	0.12 ± 0.02	0.14 ± 0.05	0.09 ± 0.11	-0.07 ± 0.07	0.03 ± 0.10	0.02 ± 0.03	0.05 ± 0.04	0.22 ± 0.08
Non-Host Stars:								
1581	-0.30 ± 0.02	-0.18 ± 0.03	-0.28 ± 0.04	-0.14 ± 0.10	-0.28 ± 0.09	-0.10 ± 0.05	-0.36 ± 0.03	-0.19 ± 0.20
3823	-0.22 ± 0.01	-0.31 ± 0.05	-0.33 ± 0.03	-0.09 ± 0.05	-0.31 ± 0.10	-0.14 ± 0.12	-0.38 ± 0.09	-0.21 ± 0.20
7570	0.01 ± 0.01	0.07 ± 0.05	-0.01 ± 0.11	-0.12 ± 0.13	-0.03 ± 0.11	0.13 ± 0.08	-0.07 ± 0.04	-0.25 ± 0.27
9280	0.29 ± 0.05	0.15 ± 0.04	0.08 ± 0.08	-0.10 ± 0.07	-0.09 ± 0.09	-0.09 ± 0.04	–	-0.19 ± 0.08

Table 2—Continued

HD	[O/H]	[Cr/H]	[Mg/H]	[Ba/H]	[Y/H]	[Zr/H]	[Eu/H]	[Nd/H]
10180	-0.04 ± 0.03	0.02 ± 0.05	-0.06 ± 0.11	-0.06 ± 0.10	-0.11 ± 0.09	-0.04 ± 0.08	-0.17 ± 0.04	0.07 ± 0.05
11112	0.02 ± 0.01	0.11 ± 0.04	-0.01 ± 0.04	-0.05 ± 0.08	-0.12 ± 0.11	0.02 ± 0.10	-0.12 ± 0.11	0.03 ± 0.06
12387	0.09 ± 0.03	-0.24 ± 0.04	-0.17 ± 0.08	-0.41 ± 0.12	-0.33 ± 0.09	-0.15 ± 0.04	-0.28 ± 0.07	-0.15 ± 0.06
18709	-0.27 ± 0.03	-0.24 ± 0.05	-0.24 ± 0.06	-0.21 ± 0.09	-0.35 ± 0.08	-0.21 ± 0.07	-0.28 ± 0.05	-0.20 ± 0.14
19632	-0.07 ± 0.03	0.07 ± 0.04	-0.13 ± 0.08	-0.04 ± 0.04	-0.24 ± 0.10	-0.20 ± 0.05	—	0.08 ± 0.10
20201	-0.13 ± 0.01	0.04 ± 0.05	-0.09 ± 0.08	0.07 ± 0.04	0.10 ± 0.08	0.13 ± 0.05	—	0.16 ± 0.08
20766	-0.28 ± 0.01	-0.21 ± 0.04	-0.26 ± 0.04	-0.40 ± 0.12	-0.40 ± 0.08	-0.27 ± 0.10	—	-0.04 ± 0.02
20794	-0.19 ± 0.01	-0.27 ± 0.04	-0.21 ± 0.09	-0.50 ± 0.13	-0.34 ± 0.09	-0.08 ± 0.08	-0.22 ± 0.04	-0.02 ± 0.03
20807	-0.27 ± 0.01	-0.26 ± 0.04	-0.26 ± 0.09	-0.39 ± 0.05	-0.28 ± 0.08	-0.13 ± 0.09	-0.30 ± 0.10	-0.03 ± 0.02
30295	0.31 ± 0.11	0.20 ± 0.05	0.06 ± 0.12	-0.02 ± 0.12	-0.10 ± 0.05	0.02 ± 0.06	—	0.03 ± 0.05
31827	0.20 ± 0.07	0.20 ± 0.05	0.19 ± 0.13	-0.19 ± 0.08	-0.13 ± 0.03	—	—	—
33811	0.01 ± 0.09	0.18 ± 0.07	0.09 ± 0.08	—	-0.15 ± 0.10	—	—	—
36108	-0.24 ± 0.02	-0.21 ± 0.03	-0.33 ± 0.02	-0.09 ± 0.05	-0.34 ± 0.09	-0.09 ± 0.04	-0.26 ± 0.06	-0.09 ± 0.06
38283	-0.12 ± 0.01	-0.20 ± 0.04	-0.19 ± 0.12	-0.32 ± 0.03	-0.23 ± 0.07	-0.24 ± 0.05	-0.21 ± 0.07	-0.31 ± 0.09
38382	-0.10 ± 0.01	-0.07 ± 0.04	-0.17 ± 0.09	0.20 ± 0.12	-0.20 ± 0.08	0.04 ± 0.10	-0.12 ± 0.11	0.00 ± 0.01
38973	-0.10 ± 0.01	-0.03 ± 0.04	-0.17 ± 0.06	-0.13 ± 0.02	-0.05 ± 0.08	0.01 ± 0.10	-0.20 ± 0.11	-0.12 ± 0.18
42902	0.06 ± 0.08	0.20 ± 0.03	-0.05 ± 0.07	—	0.21 ± 0.08	—	—	0.25 ± 0.08
43834	0.00 ± 0.02	0.07 ± 0.04	-0.1 ± 0.06	0.04 ± 0.07	-0.06 ± 0.08	0.03 ± 0.03	0.12 ± 0.05	0.09 ± 0.03
44120	-0.02 ± 0.01	-0.02 ± 0.05	0.01 ± 0.12	0.05 ± 0.09	-0.10 ± 0.12	0.03 ± 0.08	-0.18 ± 0.11	-0.04 ± 0.10
44594	0.02 ± 0.02	-0.01 ± 0.15	-0.02 ± 0.11	0.05 ± 0.12	-0.04 ± 0.10	0.09 ± 0.15	0.05 ± 0.09	0.29 ± 0.18
45289	0.00 ± 0.02	-0.03 ± 0.05	-0.02 ± 0.09	-0.06 ± 0.09	-0.16 ± 0.08	-0.05 ± 0.05	-0.28 ± 0.03	0.02 ± 0.01
45701	0.10 ± 0.02	0.09 ± 0.06	0.02 ± 0.01	0.34 ± 0.04	0.25 ± 0.09	0.35 ± 0.08	-0.12 ± 0.06	0.00 ± 0.01
52447	0.12 ± 0.02	0.10 ± 0.06	0.08 ± 0.12	0.07 ± 0.06	-0.21 ± 0.11	-0.13 ± 0.05	—	—
53705	0.16 ± 0.02	-0.20 ± 0.02	-0.2 ± 0.06	-0.26 ± 0.02	-0.24 ± 0.05	-0.32 ± 0.08	-0.12 ± 0.04	0.11 ± 0.01
53706	-0.26 ± 0.02	-0.18 ± 0.04	-0.23 ± 0.06	-0.41 ± 0.04	-0.37 ± 0.07	0.01 ± 0.05	-0.14 ± 0.06	-0.09 ± 0.07
55720	-0.17 ± 0.02	-0.20 ± 0.02	-0.23 ± 0.08	-0.41 ± 0.04	-0.28 ± 0.04	0.05 ± 0.06	-0.06 ± 0.03	0.09 ± 0.04
59468	-0.10 ± 0.05	0.10 ± 0.04	-0.1 ± 0.09	-0.12 ± 0.05	-0.10 ± 0.07	-0.08 ± 0.06	—	—
69655	-0.26 ± 0.03	-0.24 ± 0.04	-0.3 ± 0.04	-0.23 ± 0.05	-0.30 ± 0.09	0.04 ± 0.05	-0.35 ± 0.07	-0.35 ± 0.25
72769	0.10 ± 0.02	0.22 ± 0.04	0.08 ± 0.10	—	-0.04 ± 0.08	—	-0.33 ± 0.07	—
73121	-0.05 ± 0.01	-0.03 ± 0.04	-0.05 ± 0.12	0.15 ± 0.05	-0.01 ± 0.12	0.03 ± 0.03	-0.15 ± 0.02	0.03 ± 0.01
73524	-0.07 ± 0.01	0.08 ± 0.04	-0.02 ± 0.04	0.14 ± 0.08	0.16 ± 0.11	0.21 ± 0.09	0.07 ± 0.04	0.31 ± 0.05
78429	-0.04 ± 0.04	0.05 ± 0.05	-0.10 ± 0.06	-0.10 ± 0.03	-0.16 ± 0.09	0.02 ± 0.05	-0.22 ± 0.03	0.11 ± 0.08
80635	0.34 ± 0.10	0.23 ± 0.06	0.20 ± 0.02	0.01 ± 0.05	-0.03 ± 0.10	0.11 ± 0.07	-0.26 ± 0.09	-0.04 ± 0.01
82082	-0.04 ± 0.03	0.08 ± 0.05	0.07 ± 0.16	0.19 ± 0.07	0.06 ± 0.22	0.06 ± 0.05	-0.09 ± 0.04	-0.37 ± 0.05
83529A	-0.25 ± 0.04	-0.23 ± 0.04	-0.24 ± 0.07	-0.19 ± 0.10	-0.32 ± 0.09	-0.02 ± 0.06	—	-0.05 ± 0.04

Table 2—Continued

HD	[O/H]	[Cr/H]	[Mg/H]	[Ba/H]	[Y/H]	[Zr/H]	[Eu/H]	[Nd/H]
86819	-0.11 ± 0.01	-0.05 ± 0.04	-0.10 ± 0.12	-0.21 ± 0.11	-0.20 ± 0.10	-0.06 ± 0.09	-0.05 ± 0.06	-0.08 ± 0.04
88742	-0.13 ± 0.01	-0.03 ± 0.03	-0.13 ± 0.12	-0.10 ± 0.09	-0.15 ± 0.10	0.08 ± 0.06	-0.22 ± 0.08	-0.10 ± 0.07
92987	-0.06 ± 0.03	-0.01 ± 0.04	-0.06 ± 0.11	-0.25 ± 0.13	-0.27 ± 0.10	-0.01 ± 0.04	—	-0.06 ± 0.01
93385	-0.12 ± 0.02	-0.01 ± 0.03	-0.02 ± 0.19	-0.11 ± 0.11	-0.17 ± 0.10	-0.06 ± 0.04	-0.08 ± 0.08	-0.11 ± 0.18
96423	-0.05 ± 0.02	0.08 ± 0.04	0.01 ± 0.14	-0.12 ± 0.04	-0.10 ± 0.08	0.04 ± 0.11	-0.42 ± 0.08	0.08 ± 0.04
102365	-0.21 ± 0.03	-0.26 ± 0.04	-0.26 ± 0.08	-0.35 ± 0.04	-0.36 ± 0.07	-0.20 ± 0.08	-0.28 ± 0.06	-0.11 ± 0.09
105328	-0.05 ± 0.02	0.09 ± 0.04	0.05 ± 0.13	-0.30 ± 0.10	-0.06 ± 0.12	0.12 ± 0.05	-0.14 ± 0.07	0.06 ± 0.10
106453	-0.02 ± 0.01	0.07 ± 0.05	-0.13 ± 0.03	-0.05 ± 0.05	-0.06 ± 0.10	0.11 ± 0.08	—	0.07 ± 0.06
107692	-0.07 ± 0.01	0.10 ± 0.04	-0.04 ± 0.04	-0.08 ± 0.03	-0.10 ± 0.11	0.13 ± 0.04	-0.10 ± 0.05	0.05 ± 0.02
108309	0.00 ± 0.04	0.09 ± 0.04	0.01 ± 0.09	-0.07 ± 0.02	-0.17 ± 0.08	0.00 ± 0.04	-0.24 ± 0.06	-0.07 ± 0.02
114613	0.03 ± 0.01	0.09 ± 0.04	-0.04 ± 0.06	—	-0.04 ± 0.10	0.17 ± 0.04	-0.17 ± 0.04	0.05 ± 0.01
114853	-0.28 ± 0.01	-0.22 ± 0.05	-0.28 ± 0.03	-0.24 ± 0.02	-0.30 ± 0.07	-0.25 ± 0.05	-0.37 ± 0.10	-0.04 ± 0.13
122862	-0.15 ± 0.02	-0.15 ± 0.04	-0.20 ± 0.07	-0.15 ± 0.06	-0.22 ± 0.10	-0.03 ± 0.03	-0.15 ± 0.04	-0.14 ± 0.14
128620	0.15 ± 0.02	0.10 ± 0.05	0.01 ± 0.02	—	-0.09 ± 0.10	-0.10 ± 0.05	-0.09 ± 0.10	-0.07 ± 0.01
134060	-0.01 ± 0.02	0.04 ± 0.05	0.02 ± 0.14	0.02 ± 0.02	-0.04 ± 0.09	0.02 ± 0.04	-0.02 ± 0.09	0.00 ± 0.03
134330	-0.05 ± 0.04	0.04 ± 0.04	-0.12 ± 0.04	0.04 ± 0.08	-0.13 ± 0.07	—	0.03 ± 0.02	0.04 ± 0.01
140901	0.03 ± 0.03	0.09 ± 0.05	-0.04 ± 0.08	0.02 ± 0.03	0.02 ± 0.08	-0.02 ± 0.05	0.11 ± 0.04	0.14 ± 0.10
143114	-0.27 ± 0.04	-0.30 ± 0.06	-0.27 ± 0.06	-0.54 ± 0.04	-0.50 ± 0.08	-0.67 ± 0.10	-0.27 ± 0.12	-0.15 ± 0.04
147722	-0.03 ± 0.02	0.02 ± 0.03	-0.10 ± 0.05	-0.06 ± 0.01	-0.15 ± 0.10	0.02 ± 0.06	-0.01 ± 0.04	0.03 ± 0.08
155974	-0.14 ± 0.02	-0.26 ± 0.09	-0.25 ± 0.01	0.12 ± 0.18	-0.21 ± 0.12	-0.09 ± 0.05	-0.36 ± 0.07	—
161612	0.05 ± 0.01	0.11 ± 0.05	0.02 ± 0.06	0.00 ± 0.06	-0.07 ± 0.06	-0.05 ± 0.04	-0.27 ± 0.05	-0.16 ± 0.01
177565	-0.05 ± 0.03	0.06 ± 0.03	-0.12 ± 0.07	-0.25 ± 0.04	-0.13 ± 0.09	-0.04 ± 0.05	-0.03 ± 0.09	0.07 ± 0.04
183877	-0.08 ± 0.03	-0.16 ± 0.03	0.13 ± 0.09	-0.23 ± 0.03	-0.24 ± 0.08	-0.12 ± 0.07	—	0.06 ± 0.01
189567	-0.25 ± 0.02	-0.24 ± 0.04	-0.27 ± 0.03	-0.27 ± 0.05	-0.37 ± 0.08	-0.08 ± 0.02	-0.15 ± 0.08	-0.04 ± 0.03
192865	-0.05 ± 0.01	0.03 ± 0.05	0.01 ± 0.11	0.09 ± 0.02	-0.03 ± 0.17	0.00 ± 0.04	-0.19 ± 0.03	-0.16 ± 0.13
193193	-0.11 ± 0.02	-0.10 ± 0.04	-0.21 ± 0.04	-0.10 ± 0.05	-0.14 ± 0.10	0.09 ± 0.05	-0.34 ± 0.04	-0.03 ± 0.06
193307	-0.29 ± 0.01	-0.29 ± 0.04	-0.24 ± 0.11	-0.21 ± 0.10	-0.35 ± 0.11	-0.31 ± 0.09	-0.35 ± 0.04	-0.14 ± 0.07
194640	-0.11 ± 0.03	-0.02 ± 0.05	-0.12 ± 0.08	-0.17 ± 0.04	-0.15 ± 0.07	-0.09 ± 0.06	-0.27 ± 0.04	0.10 ± 0.11
196068	0.05 ± 0.04	0.20 ± 0.04	0.13 ± 0.11	-0.07 ± 0.04	-0.01 ± 0.08	0.13 ± 0.04	0.03 ± 0.03	0.11 ± 0.04
196800	0.03 ± 0.01	0.10 ± 0.03	-0.03 ± 0.09	0.28 ± 0.10	-0.05 ± 0.10	0.16 ± 0.09	0.05 ± 0.02	0.06 ± 0.07
199190	-0.02 ± 0.02	0.08 ± 0.03	-0.02 ± 0.06	-0.13 ± 0.03	-0.10 ± 0.09	0.04 ± 0.04	-0.27 ± 0.08	-0.02 ± 0.03
199288	-0.41 ± 0.01	-0.54 ± 0.04	-0.43 ± 0.02	-0.48 ± 0.03	-0.51 ± 0.09	-0.33 ± 0.04	-0.27 ± 0.07	-0.18 ± 0.04
199509	-0.34 ± 0.02	-0.35 ± 0.06	-0.36 ± 0.03	-0.29 ± 0.05	-0.31 ± 0.10	-0.11 ± 0.06	—	-0.03 ± 0.11
202628	-0.16 ± 0.05	0.00 ± 0.04	-0.14 ± 0.12	0.11 ± 0.17	-0.11 ± 0.11	0.14 ± 0.04	-0.19 ± 0.07	0.13 ± 0.01
204385	-0.33 ± 0.02	-0.01 ± 0.04	-0.07 ± 0.09	-0.16 ± 0.03	-0.15 ± 0.10	0.04 ± 0.04	—	0.05 ± 0.04

Table 2—Continued

HD	[O/H]	[Cr/H]	[Mg/H]	[Ba/H]	[Y/H]	[Zr/H]	[Eu/H]	[Nd/H]
205536	-0.13 ± 0.01	-0.01 ± 0.05	-0.16 ± 0.02	-0.24 ± 0.05	-0.20 ± 0.07	-0.14 ± 0.04	-0.23 ± 0.03	0.25 ± 0.06
207700	0.07 ± 0.04	0.05 ± 0.04	0.06 ± 0.10	-0.03 ± 0.06	-0.12 ± 0.07	-0.03 ± 0.03	-0.12 ± 0.02	0.11 ± 0.08
208998	-0.16 ± 0.01	-0.30 ± 0.04	0.19 ± 0.07	-0.39 ± 0.11	-0.41 ± 0.09	-0.24 ± 0.04	-0.41 ± 0.03	-0.15 ± 0.01
209653	-0.15 ± 0.03	-0.12 ± 0.03	-0.14 ± 0.12	-0.17 ± 0.01	-0.23 ± 0.10	-0.04 ± 0.03	-0.23 ± 0.04	-0.04 ± 0.01
210918	-0.12 ± 0.01	-0.10 ± 0.03	-0.15 ± 0.07	-0.16 ± 0.01	-0.23 ± 0.09	-0.05 ± 0.04	-0.17 ± 0.07	0.13 ± 0.05
211317	0.11 ± 0.01	0.15 ± 0.04	0.07 ± 0.08	0.02 ± 0.08	-0.06 ± 0.11	0.17 ± 0.01	0.10 ± 0.06	0.05 ± 0.11
212168	-0.13 ± 0.01	0.00 ± 0.04	-0.11 ± 0.09	-0.18 ± 0.04	-0.18 ± 0.09	0.03 ± 0.06	-0.28 ± 0.07	0.04 ± 0.10
212330	-0.06 ± 0.01	0.02 ± 0.04	-0.10 ± 0.06	0.06 ± 0.02	-0.09 ± 0.10	0.10 ± 0.09	-0.06 ± 0.04	0.20 ± 0.02
212708	0.16 ± 0.02	0.18 ± 0.05	0.00 ± 0.05	0.01 ± 0.04	-0.03 ± 0.07	0.20 ± 0.03	0.01 ± 0.01	0.23 ± 0.11
214759	0.06 ± 0.03	0.18 ± 0.06	-0.01 ± 0.03	0.11 ± 0.08	0.02 ± 0.07	-0.01 ± 0.04	-0.31 ± 0.01	0.02 ± 0.03
214953	-0.03 ± 0.01	-0.03 ± 0.03	-0.11 ± 0.09	0.06 ± 0.07	-0.08 ± 0.12	0.01 ± 0.01	0.06 ± 0.05	-0.10 ± 0.14
217958	0.13 ± 0.06	0.14 ± 0.04	0.13 ± 0.15	-0.14 ± 0.02	-0.12 ± 0.14	-0.28 ± 0.09	— 0.11	0.30 ± 0.13
219077	-0.18 ± 0.02	-0.13 ± 0.04	-0.18 ± 0.08	-0.29 ± 0.11	-0.34 ± 0.08	-0.15 ± 0.04	-0.16 ± 0.06	0.02 ± 0.01
220507	0.04 ± 0.03	-0.03 ± 0.04	-0.01 ± 0.10	-0.23 ± 0.13	-0.24 ± 0.09	-0.06 ± 0.08	-0.17 ± 0.03	0.03 ± 0.01
221420	0.11 ± 0.02	0.20 ± 0.04	0.08 ± 0.05	-0.01 ± 0.09	-0.01 ± 0.10	0.17 ± 0.04	0.05 ± 0.03	0.21 ± 0.11
223171	0.03 ± 0.02	0.04 ± 0.04	-0.08 ± 0.04	0.04 ± 0.02	-0.10 ± 0.10	0.05 ± 0.05	-0.01 ± 0.03	0.01 ± 0.06

Table 3. Stellar Abundances normalized to 10^6 Si atoms. Solar values are based on the abundances in Asplund et al. (2005)

HD	Fe	O	Mg	Cr	Y	Zr	Ba	Nd	Eu
Host Stars:									
Solar	8.71×10^5	1.41×10^7	1.05×10^6	1.35×10^4	5.01	12.02	4.57	0.87	0.10
2039	1.00×10^6	9.12×10^6	7.76×10^5	1.26×10^4	3.63	7.24	3.31	0.78	0.05
4308	8.32×10^5	1.48×10^7	8.91×10^5	1.02×10^4	2.57	11.22	2.34	0.83	0.13
10647	9.77×10^5	1.70×10^7	1.23×10^6	1.62×10^4	6.17	18.88	8.91	0.76	0.09
13445	8.32×10^5	1.78×10^7	1.17×10^6	1.86×10^4	4.68	—	3.16	1.57	0.08
17051	7.94×10^5	1.15×10^7	6.31×10^5	1.32×10^4	4.07	13.80	5.62	0.83	0.07
23079	1.07×10^6	9.77×10^6	5.89×10^5	1.12×10^4	3.89	12.88	3.31	0.93	0.08
20782	7.94×10^5	5.25×10^6	1.17×10^6	1.91×10^4	2.57	5.75	—	0.58	0.05
30177	6.76×10^5	1.05×10^7	4.57×10^5	1.00×10^4	2.00	4.07	1.32	0.55	—
39091	1.05×10^6	—	1.12×10^6	1.62×10^4	—	9.33	—	0.68	0.07
70642	1.00×10^6	1.10×10^7	8.32×10^5	1.41×10^4	4.17	13.49	2.95	—	0.06
73526	6.17×10^5	9.33×10^6	6.76×10^5	9.77×10^3	2.29	11.22	2.82	0.62	0.09
75289	6.76×10^5	8.51×10^6	6.17×10^5	1.17×10^4	3.09	13.80	3.16	1.05	0.07
83443	4.68×10^5	8.32×10^6	4.79×10^5	8.32×10^3	1.82	3.39	—	0.31	—
102117	6.76×10^5	9.77×10^6	6.31×10^5	1.15×10^4	2.57	10.47	3.02	0.63	—
108147	8.71×10^5	1.26×10^7	9.33×10^5	1.58×10^4	4.90	10.79	5.25	0.85	0.11
117618	0.76×10^6	1.10×10^7	8.71×10^5	1.10×10^4	3.72	11.75	5.37	1.07	0.08
134987	6.17×10^5	1.05×10^7	8.32×10^5	1.29×10^4	3.63	9.33	4.47	0.78	0.05
142415	1.45×10^6	1.38×10^7	8.51×10^5	1.32×10^4	8.13	—	9.33	1.77	0.10
154857	8.91×10^5	1.91×10^7	1.26×10^6	1.62×10^4	4.90	19.05	6.76	1.62	0.10
160691	6.46×10^5	9.77×10^6	7.08×10^5	1.05×10^4	2.45	9.33	2.29	0.65	0.03
164427	6.61×10^5	1.05×10^7	6.92×10^5	1.23×10^4	2.63	7.41	2.51	0.89	0.06
179949	9.12×10^5	1.20×10^7	9.12×10^5	1.48×10^4	5.75	18.20	2.14	0.93	0.07
187085	7.59×10^5	1.12×10^7	6.76×10^5	1.17×10^4	3.89	12.88	4.57	0.74	0.04
196050	5.89×10^5	—	8.91×10^5	1.17×10^4	3.39	10.23	3.09	0.50	0.04
208487	9.12×10^5	1.41×10^7	1.02×10^6	1.74×10^4	5.37	15.85	4.90	1.05	0.09
213240	0.78×10^6	1.02×10^7	6.92×10^5	1.20×10^4	3.55	10.72	3.89	1.07	0.10
216435	6.61×10^5	1.41×10^7	9.77×10^5	1.45×10^4	4.79	14.45	5.13	0.66	0.06
216437	6.61×10^5	1.05×10^7	7.24×10^5	1.05×10^4	3.02	7.08	2.19	0.81	0.06
Non-Host Stars:									
1581	7.24×10^5	9.77×10^6	7.59×10^5	1.23×10^4	3.63	13.18	4.57	0.78	0.06
3823	7.24×10^5	1.41×10^7	8.13×10^5	1.10×10^4	4.07	14.45	6.17	0.89	0.07
7570	0.68×10^6	9.55×10^6	6.76×10^5	1.05×10^4	3.09	10.72	2.29	0.32	0.06

Table 3—Continued

HD	Fe	O	Mg	Cr	Y	Zr	Ba	Nd	Eu
9280	0.62 x10 ⁶	1.45 x10 ⁷	6.61 x10 ⁵	1.00 x10 ⁴	2.14	5.13	1.91	0.30	—
10180	7.41 x10 ⁵	1.12 x10 ⁷	7.94 x10 ⁵	1.23 x10 ⁴	3.39	9.55	3.47	0.89	0.06
11112	0.65 x10 ⁶	9.33 x10 ⁶	6.46 x10 ⁵	1.10 x10 ⁴	2.40	7.94	2.57	0.59	0.05
12387	5.89 x10 ⁵	2.09 x10 ⁷	8.51 x10 ⁵	9.33 x10 ³	2.82	10.23	2.14	0.74	0.06
18709	7.76 x10 ⁵	1.15 x10 ⁷	9.12 x10 ⁵	1.17 x10 ⁴	3.39	11.22	4.27	0.83	0.08
19632	6.31 x10 ⁵	1.07 x10 ⁷	6.92 x10 ⁵	1.41 x10 ⁴	2.57	6.76	3.72	0.93	—
20201	7.41 x10 ⁵	8.51 x10 ⁶	6.92 x10 ⁵	1.20 x10 ⁴	5.13	13.18	4.37	1.02	—
20766	7.59 x10 ⁵	1.07 x10 ⁷	8.32 x10 ⁵	1.20 x10 ⁴	2.88	9.33	2.63	1.15	—
20794	6.03 x10 ⁵	1.32 x10 ⁷	9.33 x10 ⁵	1.05 x10 ⁴	3.31	14.45	2.09	1.20	0.09
20807	7.41 x10 ⁵	1.15 x10 ⁷	8.71 x10 ⁵	1.12 x10 ⁴	3.98	13.49	2.82	1.23	0.08
30295	0.59 x10 ⁶	1.38 x10 ⁷	5.75 x10 ⁵	1.02 x10 ⁴	1.91	6.03	2.09	0.45	—
31827	0.42 x10 ⁶	6.76 x10 ⁶	4.90 x10 ⁵	6.46 x10 ³	1.12	—	0.89	—	—
33811	0.62 x10 ⁶	7.24 x10 ⁶	6.46 x10 ⁵	1.02 x10 ⁴	1.78	—	—	—	—
36108	7.76 x10 ⁵	1.26 x10 ⁷	7.59 x10 ⁵	1.29 x10 ⁴	3.55	15.14	5.75	1.10	0.09
38283	7.08 x10 ⁵	1.51 x10 ⁷	9.55 x10 ⁵	1.20 x10 ⁴	4.17	9.77	3.09	0.60	0.09
38382	7.24 x10 ⁵	1.15 x10 ⁷	7.24 x10 ⁵	1.17 x10 ⁴	3.24	13.49	7.41	0.89	0.08
38973	7.24 x10 ⁵	1.10 x10 ⁷	6.92 x10 ⁵	1.23 x10 ⁴	4.37	12.02	3.31	0.65	0.06
42902	0.62 x10 ⁶	7.76 x10 ⁶	4.47 x10 ⁵	1.02 x10 ⁴	3.89	—	—	0.74	—
43834	0.74 x10 ⁶	1.05 x10 ⁷	6.17 x10 ⁵	1.17 x10 ⁴	3.24	9.55	3.72	0.79	0.10
44120	7.24 x10 ⁵	1.10 x10 ⁷	8.71 x10 ⁵	1.05 x10 ⁴	3.24	10.47	4.17	0.65	0.05
44594	6.76 x10 ⁵	1.05 x10 ⁷	7.08 x10 ⁵	9.33 x10 ³	3.24	10.47	3.63	1.20	0.08
45289	6.92 x10 ⁵	1.29 x10 ⁷	9.12 x10 ⁵	1.15 x10 ⁴	3.16	9.77	3.63	0.83	0.05
45701	0.68 x10 ⁶	1.17 x10 ⁷	7.24 x10 ⁵	1.10 x10 ⁴	5.89	17.78	6.61	0.58	0.05
52447	0.60 x10 ⁶	1.07 x10 ⁷	7.24 x10 ⁵	9.77 x10 ³	1.78	5.13	3.09	—	—
53705	6.76 x10 ⁵	2.69 x10 ⁷	8.71 x10 ⁵	1.12 x10 ⁴	3.80	7.59	3.31	1.48	0.10
53706	6.92 x10 ⁵	1.10 x10 ⁷	8.71 x10 ⁵	1.26 x10 ⁴	3.02	17.38	2.51	1.00	0.10
55720	6.17 x10 ⁵	1.26 x10 ⁷	8.13 x10 ⁵	1.12 x10 ⁴	3.47	17.78	2.34	1.41	0.12
59468	8.13 x10 ⁵	9.33 x10 ⁶	6.92 x10 ⁵	1.41 x10 ⁴	3.31	8.32	2.88	—	—
69655	7.24 x10 ⁵	1.07 x10 ⁷	7.24 x10 ⁵	1.07 x10 ⁴	3.47	18.20	3.72	0.54	0.06
72769	0.55 x10 ⁶	8.13 x10 ⁶	5.75 x10 ⁵	1.02 x10 ⁴	2.09	—	—	—	0.02
73121	7.41 x10 ⁵	1.12 x10 ⁷	8.32 x10 ⁵	1.12 x10 ⁴	4.37	11.48	5.75	0.83	0.06
73524	0.81 x10 ⁶	9.12 x10 ⁶	7.59 x10 ⁵	1.23 x10 ⁴	5.50	14.79	4.79	1.35	0.09
78429	7.41 x10 ⁵	1.07 x10 ⁷	6.92 x10 ⁵	1.26 x10 ⁴	2.88	10.47	3.02	0.93	0.05
80635	0.48 x10 ⁶	1.12 x10 ⁷	6.03 x10 ⁵	8.32 x10 ³	1.70	5.62	1.70	0.29	0.02
82082	6.61 x10 ⁵	1.05 x10 ⁷	1.00 x10 ⁶	1.32 x10 ⁴	4.68	11.22	5.75	0.30	0.07

Table 3—Continued

HD	Fe	O	Mg	Cr	Y	Zr	Ba	Nd	Eu
83529A	8.71 x10 ⁵	1.26 x10 ⁷	9.55 x10 ⁵	1.26 x10 ⁴	3.80	18.20	4.68	1.23	—
86819	7.24 x10 ⁵	1.12 x10 ⁷	8.51 x10 ⁵	1.23 x10 ⁴	3.24	10.72	2.88	0.74	0.09
88742	7.59 x10 ⁵	1.15 x10 ⁷	8.51 x10 ⁵	1.38 x10 ⁴	3.89	15.85	3.98	0.76	0.07
92987	6.17 x10 ⁵	1.05 x10 ⁷	7.76 x10 ⁵	1.12 x10 ⁴	2.29	10.00	2.19	0.65	—
93385	7.08 x10 ⁵	1.05 x10 ⁷	9.77 x10 ⁵	1.29 x10 ⁴	3.31	10.23	3.47	0.66	0.08
96423	6.76 x10 ⁵	9.55 x10 ⁶	8.13 x10 ⁵	1.23 x10 ⁴	3.02	10.00	2.63	0.79	0.03
102365	7.08 x10 ⁵	1.35 x10 ⁷	8.91 x10 ⁵	1.15 x10 ⁴	3.39	11.75	3.16	1.05	0.08
105328	6.76 x10 ⁵	8.71 x10 ⁶	8.13 x10 ⁵	1.15 x10 ⁴	3.02	10.96	1.58	0.69	0.05
106453	7.24 x10 ⁵	1.15 x10 ⁷	6.61 x10 ⁵	1.35 x10 ⁴	3.72	13.18	3.47	0.87	—
107692	6.03 x10 ⁵	9.12 x10 ⁶	7.24 x10 ⁵	1.29 x10 ⁴	3.02	12.30	2.88	0.74	0.06
108309	5.89 x10 ⁵	1.05 x10 ⁷	7.94 x10 ⁵	1.23 x10 ⁴	2.51	8.91	2.88	0.55	0.04
114613	0.65 x10 ⁶	9.77 x10 ⁶	6.17 x10 ⁵	1.07 x10 ⁴	2.95	11.48	—	0.63	0.04
114853	9.33 x10 ⁵	1.20 x10 ⁷	8.91 x10 ⁵	1.32 x10 ⁴	4.07	10.96	4.27	1.29	0.07
122862	7.59 x10 ⁵	1.23 x10 ⁷	8.13 x10 ⁵	1.17 x10 ⁴	3.72	13.80	3.98	0.78	0.09
128620	5.62 x10 ⁵	1.20 x10 ⁷	6.46 x10 ⁵	1.02 x10 ⁴	2.45	5.75	—	0.45	0.05
134060	7.41 x10 ⁵	1.10 x10 ⁷	8.71 x10 ⁵	1.17 x10 ⁴	3.63	10.00	3.80	0.69	0.08
134330	7.08 x10 ⁵	1.07 x10 ⁷	6.76 x10 ⁵	1.26 x10 ⁴	3.16	—	4.27	0.81	0.09
140901	7.59 x10 ⁵	1.17 x10 ⁷	7.41 x10 ⁵	1.29 x10 ⁴	4.07	8.91	3.72	0.93	0.10
143114	6.31 x10 ⁵	1.38 x10 ⁷	1.02 x10 ⁶	1.23 x10 ⁴	2.88	4.68	2.40	1.12	0.10
147722	6.76 x10 ⁵	1.12 x10 ⁷	7.08 x10 ⁵	1.20 x10 ⁴	3.02	10.72	3.39	0.79	0.09
155974	7.76 x10 ⁵	1.45 x10 ⁷	8.32 x10 ⁵	1.05 x10 ⁴	4.37	13.80	8.51	—	0.06
161612	0.68 x10 ⁶	1.07 x10 ⁷	7.41 x10 ⁵	1.17 x10 ⁴	2.88	7.24	3.09	0.41	0.04
177565	6.31 x10 ⁵	1.07 x10 ⁷	6.76 x10 ⁵	1.32 x10 ⁴	3.16	9.33	2.19	0.87	0.08
183877	6.31 x10 ⁵	1.29 x10 ⁷	1.55 x10 ⁶	1.02 x10 ⁴	3.16	10.00	2.95	1.10	—
189567	7.08 x10 ⁵	1.15 x10 ⁷	8.13 x10 ⁵	1.12 x10 ⁴	3.09	14.45	3.55	1.15	0.10
192865	7.59 x10 ⁵	1.17 x10 ⁷	1.00 x10 ⁶	1.35 x10 ⁴	4.37	11.22	5.25	0.56	0.06
193193	7.94 x10 ⁵	1.23 x10 ⁷	7.24 x10 ⁵	1.20 x10 ⁴	4.07	16.60	4.07	0.91	0.05
193307	10.00 x10 ⁵	1.55 x10 ⁷	1.29 x10 ⁶	1.48 x10 ⁴	4.79	12.59	6.03	1.35	0.10
194640	7.59 x10 ⁵	1.07 x10 ⁷	7.76 x10 ⁵	1.26 x10 ⁴	3.47	9.55	3.02	1.07	0.05
196068	0.63 x10 ⁶	7.76 x10 ⁶	6.92 x10 ⁵	1.05 x10 ⁴	2.40	7.94	1.91	0.55	0.05
196800	6.92 x10 ⁵	1.07 x10 ⁷	6.92 x10 ⁵	1.20 x10 ⁴	3.16	12.30	6.17	0.71	0.08
199190	6.76 x10 ⁵	9.55 x10 ⁶	7.08 x10 ⁵	1.15 x10 ⁴	2.82	9.33	2.40	0.59	0.04
199288	26.30 x10 ⁵	1.51 x10 ⁷	1.07 x10 ⁶	1.07 x10 ⁴	4.27	15.49	4.17	1.58	0.15
199509	7.76 x10 ⁵	1.12 x10 ⁷	7.94 x10 ⁵	1.05 x10 ⁴	4.27	16.22	4.07	1.41	—
202628	7.41 x10 ⁵	1.07 x10 ⁷	8.32 x10 ⁵	1.48 x10 ⁴	4.27	18.20	6.46	1.29	0.07

Table 3—Continued

HD	Fe	O	Mg	Cr	Y	Zr	Ba	Nd	Eu
204385	7.24×10^5	6.17×10^6	8.32×10^5	1.23×10^4	3.31	12.30	2.95	0.91	—
205536	6.76×10^5	9.77×10^6	6.76×10^5	1.23×10^4	2.95	8.13	2.45	1.45	0.06
207700	6.61×10^5	1.17×10^7	8.51×10^5	1.07×10^4	2.69	7.94	3.02	0.79	0.05
208998	5.75×10^5	1.41×10^7	2.34×10^6	9.77×10^3	2.82	10.00	2.69	0.89	0.06
209653	7.41×10^5	1.20×10^7	9.12×10^5	1.23×10^4	3.55	13.18	3.72	0.95	0.07
210918	7.59×10^5	1.23×10^7	8.51×10^5	1.23×10^4	3.39	12.30	3.63	1.35	0.08
211317	0.62×10^6	1.02×10^7	6.92×10^5	1.07×10^4	2.45	10.00	2.69	0.55	0.07
212168	7.76×10^5	1.05×10^7	8.13×10^5	1.35×10^4	3.31	12.88	3.02	0.95	0.05
212330	8.13×10^5	1.15×10^7	7.76×10^5	1.32×10^4	3.80	14.13	4.90	1.29	0.08
212708	0.62×10^6	1.07×10^7	5.50×10^5	1.07×10^4	2.45	10.00	2.45	0.78	0.05
214759	0.63×10^6	8.91×10^6	5.62×10^5	1.12×10^4	2.88	6.46	3.24	0.50	0.03
214953	7.24×10^5	1.26×10^7	7.76×10^5	1.20×10^4	3.98	11.75	5.01	0.66	0.11
217958	0.51×10^6	9.12×10^6	6.76×10^5	8.91×10^3	1.82	3.02	1.58	0.83	—
219077	6.61×10^5	1.15×10^7	8.51×10^5	1.23×10^4	2.82	10.47	2.88	1.12	0.09
220507	6.61×10^5	1.41×10^7	9.33×10^5	1.15×10^4	2.63	9.55	2.45	0.85	0.06
221420	0.60×10^6	8.51×10^6	5.89×10^5	1.00×10^4	2.29	8.32	2.09	0.66	0.05
223171	7.24×10^5	1.23×10^7	7.08×10^5	1.20×10^4	3.24	10.96	4.07	0.72	0.08

Table 4. C and Si Abundances from Bond et al. (2006).

HD	[C/H]	C atoms	[Si/H]	HD	[C/H]	C atoms	[Si/H]
Host Stars:				Non-Host Stars (cont.):			
Solar		7.59 x10 ⁶		31827	0.37 ± 0.12	5.37 x10 ⁶	0.52 ± 0.14
2039	0.22 ± 0.16	6.61 x10 ⁶	0.28 ± 0.12	33811	0.03 ± 0.11	4.07 x10 ⁶	0.30 ± 0.06
4308	-0.16 ± 0.08	7.41 x10 ⁶	-0.15 ± 0.06	36108	-0.13 ± 0.06	8.71 x10 ⁶	-0.19 ± 0.05
10647	-0.14 ± 0.06	9.12 x10 ⁶	-0.22 ± 0.09	38283	-0.07 ± 0.03	9.12 x10 ⁶	-0.15 ± 0.03
13445	-0.17 ± 0.10	1.07 x10 ⁷	-0.32 ± 0.10	38382	0.03 ± 0.05	8.32 x10 ⁶	-0.01 ± 0.04
17051	0.09 ± 0.11	7.59 x10 ⁶	0.09 ± 0.07	38973	-0.01 ± 0.06	7.24 x10 ⁶	0.01 ± 0.09
23079	-0.07 ± 0.10	7.76 x10 ⁶	-0.08 ± 0.05	42902	0.30 ± 0.13	7.24 x10 ⁶	0.32 ± 0.08
20782	0.01 ± 0.12	8.32 x10 ⁶	-0.03 ± 0.05	43834	0.04 ± 0.09	6.17 x10 ⁶	0.13 ± 0.09
30177	0.27 ± 0.09	5.25 x10 ⁶	0.43 ± 0.08	44120	0.13 ± 0.10	8.32 x10 ⁶	0.09 ± 0.07
39091	0.03 ± 0.06	6.92 x10 ⁶	0.07 ± 0.03	44594	0.08 ± 0.05	6.46 x10 ⁶	0.15 ± 0.09
70642	–	–	0.19 ± 0.11	45289	0.12 ± 0.13	9.12 x10 ⁶	0.04 ± 0.05
73526	0.22 ± 0.09	6.92 x10 ⁶	0.26 ± 0.08	45701	0.24 ± 0.13	8.71 x10 ⁶	0.18 ± 0.07
75289	0.12 ± 0.18	5.89 x10 ⁶	0.23 ± 0.05	52447	0.30 ± 0.18	8.71 x10 ⁶	0.24 ± 0.13
83443	0.30 ± 0.23	4.79 x10 ⁶	0.50 ± 0.02	53705	-0.08 ± 0.11	8.32 x10 ⁶	-0.12 ± 0.09
102117	0.33 ± 0.13	8.32 x10 ⁶	0.29 ± 0.13	53706	-0.09 ± 0.08	8.71 x10 ⁶	-0.15 ± 0.08
108147	-0.05 ± 0.06	7.08 x10 ⁶	-0.02 ± 0.11	55720	-0.13 ± 0.14	7.41 x10 ⁶	-0.12 ± 0.09
117618	0.01 ± 0.15	7.41 x10 ⁶	0.02 ± 0.06	59468	0.07 ± 0.08	7.41 x10 ⁶	0.08 ± 0.09
134987	0.29 ± 0.10	7.08 x10 ⁶	0.32 ± 0.05	69655	-0.12 ± 0.09	7.94 x10 ⁶	-0.14 ± 0.10
142415	0.01 ± 0.04	1.23 x10 ⁷	-0.2 ± 0.13	72769	–	–	0.34 ± 0.13
154857	-0.28 ± 0.07	7.59 x10 ⁶	-0.28 ± 0.11	73121	0.11 ± 0.08	8.71 x10 ⁶	0.05 ± 0.10
160691	0.31 ± 0.12	7.59 x10 ⁶	0.31 ± 0.07	73524	0.11 ± 0.06	7.41 x10 ⁶	0.12 ± 0.04
164427	0.14 ± 0.09	8.13 x10 ⁶	0.11 ± 0.08	78429	0.02 ± 0.05	6.61 x10 ⁶	0.08 ± 0.09
179949	0.15 ± 0.02	8.51 x10 ⁶	0.10 ± 0.11	80635	0.33 ± 0.19	5.89 x10 ⁶	0.44 ± 0.21
187085	0.08 ± 0.04	8.13 x10 ⁶	0.05 ± 0.03	82082	0.02 ± 0.04	6.46 x10 ⁶	0.09 ± 0.06
196050	0.20 ± 0.11	6.61 x10 ⁶	0.26 ± 0.06	83529A	-0.2 ± 0.12	7.59 x10 ⁶	-0.2 ± 0.14
208487	0.02 ± 0.02	9.77 x10 ⁶	-0.09 ± 0.10	86819	0.01 ± 0.06	7.94 x10 ⁶	-0.01 ± 0.06
213240	0.18 ± 0.08	8.32 x10 ⁶	0.14 ± 0.06	88742	0.00 ± 0.06	8.32 x10 ⁶	-0.04 ± 0.07
216435	0.17 ± 0.09	6.92 x10 ⁶	0.21 ± 0.07	92987	–	–	0.07 ± 0.06
216437	0.23 ± 0.10	7.24 x10 ⁶	0.25 ± 0.08	93385	0.03 ± 0.10	7.94 x10 ⁶	0.01 ± 0.07
				96423	–	–	0.12 ± 0.07
Non-Host Stars:				102365	-0.18 ± 0.15	7.76 x10 ⁶	-0.19 ± 0.12
1581	-0.28 ± 0.10	5.50 x10 ⁶	-0.14 ± 0.07	105328	0.13 ± 0.08	7.08 x10 ⁶	0.16 ± 0.09
3823	-0.22 ± 0.08	7.59 x10 ⁶	-0.22 ± 0.15	106453	-0.1 ± 0.09	5.13 x10 ⁶	0.07 ± 0.09
7570	0.20 ± 0.14	7.94 x10 ⁶	0.18 ± 0.10	107692	0.00 ± 0.05	5.75 x10 ⁶	0.12 ± 0.08
9280	0.38 ± 0.19	9.55 x10 ⁶	0.28 ± 0.12	108309	0.14 ± 0.06	7.76 x10 ⁶	0.13 ± 0.05
10180	0.06 ± 0.11	7.59 x10 ⁶	0.06 ± 0.04	114613	–	–	0.19 ± 0.06
11112	0.18 ± 0.09	7.24 x10 ⁶	0.20 ± 0.07	114853	-0.17 ± 0.09	8.32 x10 ⁶	-0.21 ± 0.09
12387	-0.05 ± 0.09	8.13 x10 ⁶	-0.08 ± 0.05	122862	-0.08 ± 0.12	7.76 x10 ⁶	-0.09 ± 0.08
18709	-0.26 ± 0.09	6.31 x10 ⁶	-0.18 ± 0.05	128620	–	–	0.22 ± 0.07
19632	-0.03 ± 0.09	6.31 x10 ⁶	0.05 ± 0.04	134060	0.05 ± 0.06	6.76 x10 ⁶	0.10 ± 0.07
20201	-0.04 ± 0.12	5.62 x10 ⁶	0.09 ± 0.05	134330	-0.04 ± 0.13	5.89 x10 ⁶	0.07 ± 0.05
20766	-0.19 ± 0.11	7.08 x10 ⁶	-0.16 ± 0.09	140901	0.03 ± 0.05	6.31 x10 ⁶	0.11 ± 0.09
20794	-0.08 ± 0.09	9.12 x10 ⁶	-0.16 ± 0.07	143114	-0.18 ± 0.11	9.12 x10 ⁶	-0.26 ± 0.09
20807	-0.19 ± 0.12	7.41 x10 ⁶	-0.18 ± 0.08	147722	0.05 ± 0.08	7.24 x10 ⁶	0.07 ± 0.08
30295	–	–	0.32 ± 0.16	155974	-0.1 ± 0.12	8.51 x10 ⁶	-0.15 ± 0.07

Table 4—Continued

HD	[C/H]	C atoms	[Si/H]	HD	[C/H]	C atoms	[Si/H]
161612	0.07 ± 0.09	6.03×10^6	0.17 ± 0.07	207700	0.13 ± 0.11	7.24×10^6	0.15 ± 0.01
177565	0.09 ± 0.08	7.94×10^6	0.07 ± 0.06	209653	-0.08 ± 0.13	7.59×10^6	-0.08 ± 0.07
183877	-0.01 ± 0.08	8.13×10^6	-0.04 ± 0.05	208998	-0.08 ± 0.06	9.12×10^6	-0.16 ± 0.11
189567	-0.33 ± 0.13	5.13×10^6	-0.16 ± 0.09	210918	-0.02 ± 0.08	8.32×10^6	-0.06 ± 0.05
192865	0.06 ± 0.15	8.13×10^6	0.03 ± 0.11	211317	0.25 ± 0.09	7.59×10^6	0.25 ± 0.08
193193	-0.07 ± 0.11	7.24×10^6	-0.05 ± 0.09	212168	-0.19 ± 0.12	4.90×10^6	0.00 ± 0.07
193307	-0.33 ± 0.19	7.59×10^6	-0.33 ± 0.05	212330	–	–	0.03 ± 0.06
194640	–	–	0.01 ± 0.08	212708	0.27 ± 0.14	7.41×10^6	0.28 ± 0.08
196068	0.16 ± 0.09	5.37×10^6	0.31 ± 0.14	214759	–	–	0.26 ± 0.11
196800	0.36 ± 0.21	12.30×10^6	0.15 ± 0.14	214953	0.09 ± 0.06	8.91×10^6	0.02 ± 0.07
199190	0.21 ± 0.13	8.71×10^6	0.15 ± 0.08	217958	–	–	0.32 ± 0.07
199288	-0.41 ± 0.15	8.13×10^6	-0.44 ± 0.10	219077	–	–	-0.09 ± 0.06
199509	–	–	-0.24 ± 0.10	220507	0.15 ± 0.09	9.77×10^6	0.04 ± 0.08
202628	-0.15 ± 0.10	5.89×10^6	-0.04 ± 0.09	221420	–	–	0.33 ± 0.05
204385	0.07 ± 0.13	8.32×10^6	0.03 ± 0.07	223171	0.19 ± 0.13	9.55×10^6	0.09 ± 0.06
205536	-0.03 ± 0.08	6.61×10^6	0.03 ± 0.06				

Table 5. Mean difference from published abundances

Study	Element	Difference	Sample Size
Berião et al. (2005)	Mg	-0.18 ± 0.02	29
Gilli et al. (2006)	Cr	0.00 ± 0.02	28
	Mg	-0.18 ± 0.02	29
Bodaghee et al (2003)	Cr	0.02 ± 0.01	25
Ecuillon et al (2006)	O	0.11 ± 0.07	8
Gonzalez & Laws (2007)	O	-0.03 ± 0.04	4
	Eu	-0.22 ± 0.16	4

Table 6. Statistical analysis of abundance distributions. Difference is defined as host star abundance – non-host star abundance. Numbers in parentheses indicate the sample size. K–S test values are the confidence percentages that the two samples do *not* come from the same parent population.

	Non-Planetary Hosts	Planetary Hosts	Difference	K–S Result		Non-Planetary Hosts	Planetary Hosts	Difference	K–S Result
O:					Zr:				
Mean	-0.06 ± 0.02 (90)	$+0.00 \pm 0.03$ (27)	0.06	91.2	Mean	-0.03 ± 0.02 (85)	$+0.06 \pm 0.03$ (26)	0.09	97.5
Median	-0.05 ± 0.02	$+0.00^{+0.04}_{-0.03}$	0.05		Median	$-0.01^{+0.03}_{-0.02}$	$+0.05^{+0.03}_{-0.06}$	0.06	
Std. Dev.	0.15	0.17			Std. Dev.	0.15	0.16		
Mg:					Ba:				
Mean	-0.09 ± 0.01 (90)	-0.02 ± 0.03 (28)	0.07	96.82	Mean	-0.11 ± 0.02 (85)	-0.01 ± 0.04 (26)	0.10	98.2
Median	$-0.10^{+0.04}_{-0.01}$	$+0.01^{+0.06}_{-0.07}$	0.11		Median	-0.11 ± 0.02	$+0.05^{+0.04}_{-0.05}$	0.16	
Std. Dev.	0.14	0.16			Std. Dev.	0.18	0.19		
Cr:					Eu:				
Mean	-0.03 ± 0.02 (90)	$+0.08 \pm 0.03$ (28)	0.11	99.45	Mean	-0.16 ± 0.02 (73)	-0.10 ± 0.03 (26)	0.06	96.16
Median	$+0.00^{+0.04}_{-0.01}$	$+0.12^{+0.03}_{-0.02}$	0.12		Median	$-0.17^{+0.03}_{-0.04}$	$-0.09^{+0.04}_{-0.05}$	0.08	
Std. Dev.	0.16	0.17			Std. Dev.	0.14	0.15		
Y:					Nd:				
Mean	-0.16 ± 0.01 (90)	-0.05 ± 0.03 (27)	0.11	99.99	Mean	$+0.00 \pm 0.02$ (84)	$+0.06 \pm 0.03$ (27)	0.06	97.85
Median	-0.15 ± 0.03	$+0.00 \pm 0.02$	0.15		Median	$+0.01 \pm 0.03$	$+0.09^{+0.01}_{-0.05}$	0.08	
Std. Dev.	0.14	0.16			Std. Dev.	0.14	0.15		

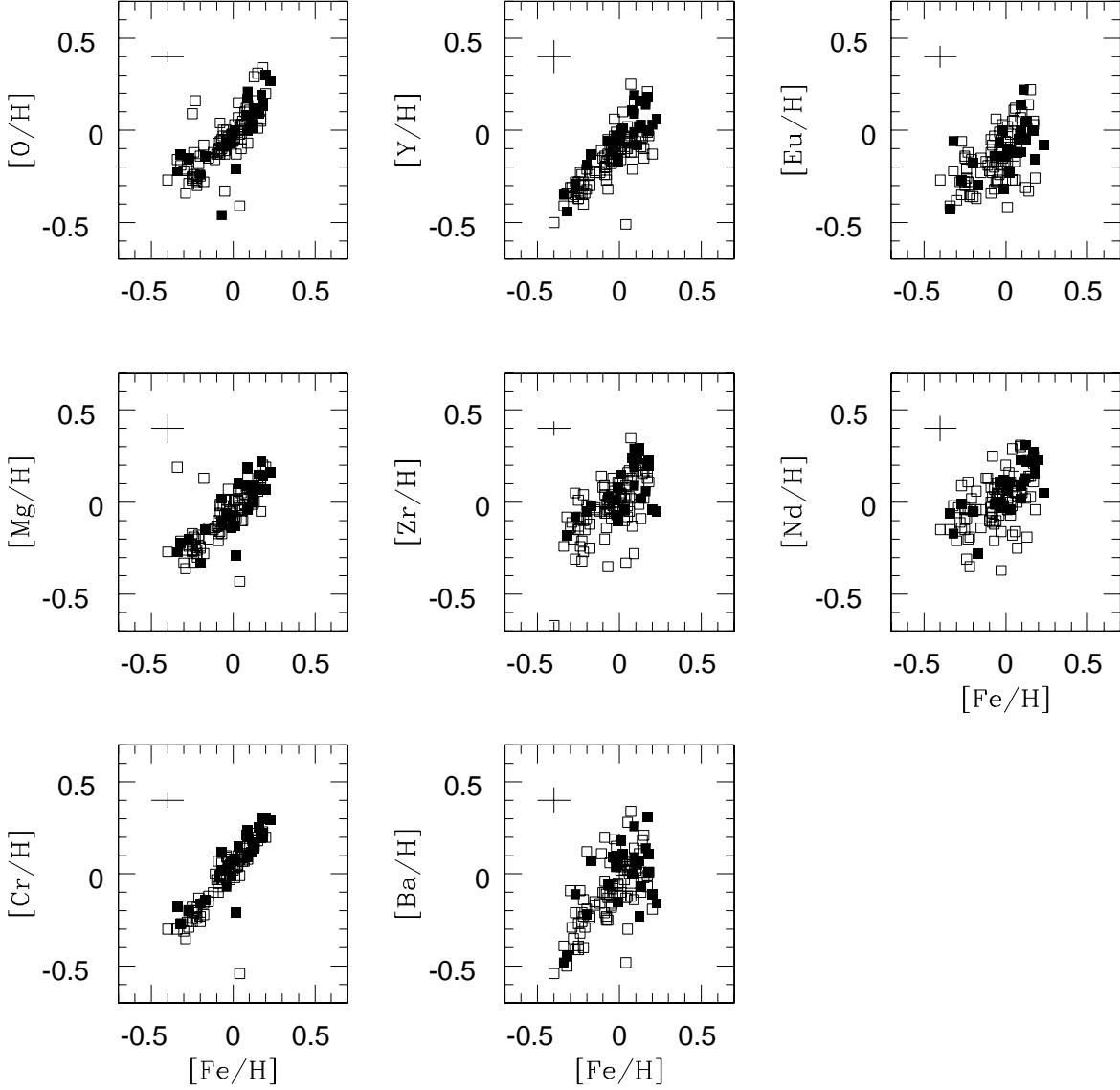


Fig. 1.— $[X/H]$ vs. $[Fe/H]$ plots for all elements studied. Open squares represent non-host stars and filled squares represent host stars. Typical error bars are shown in the upper left of each panel. *Left Column:* O, Mg and Cr. *Center Column:* Y, Zr and Ba. *Right Column:* Eu and Nd.

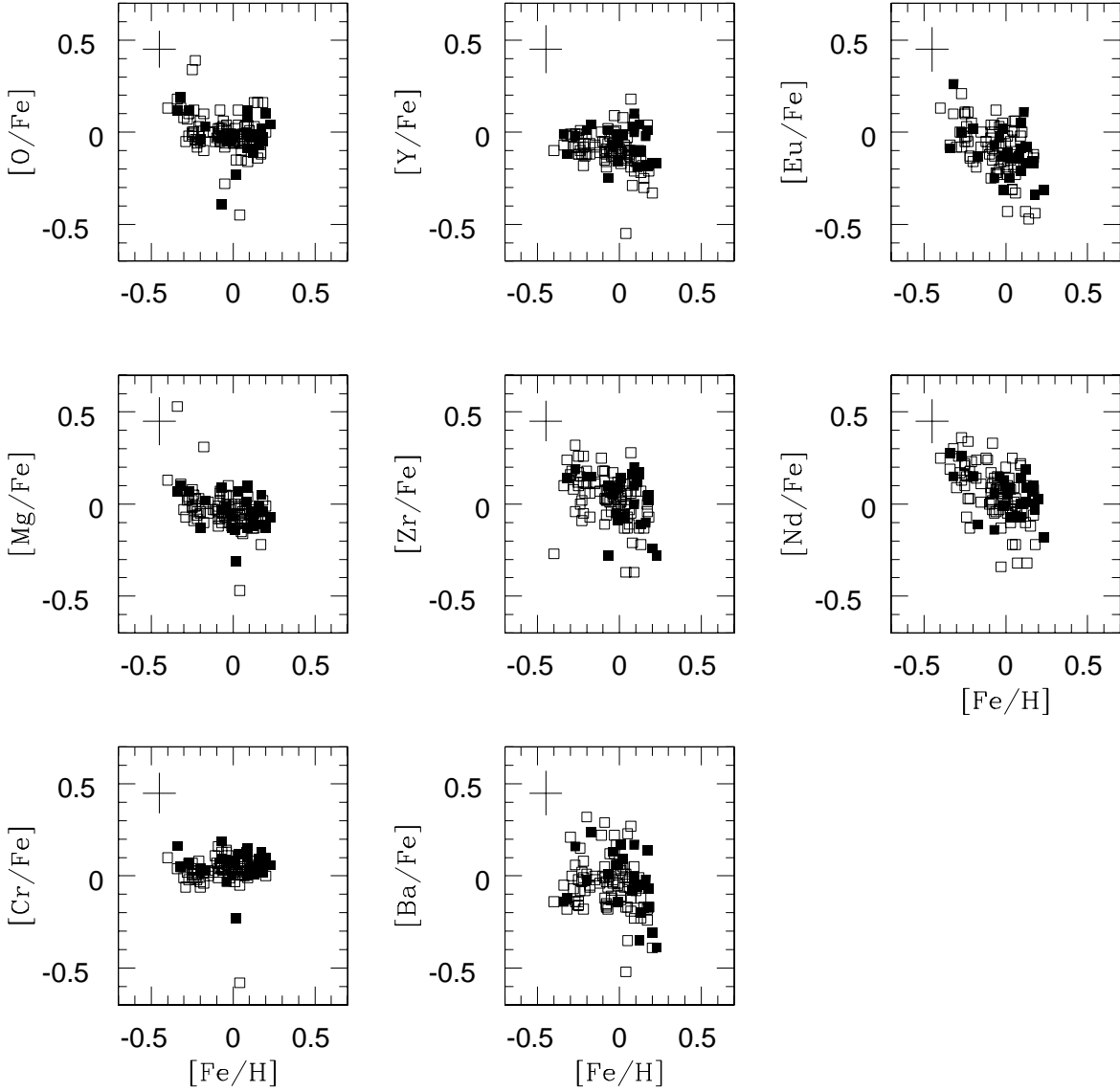


Fig. 2.— $[X/Fe]$ vs. $[Fe/H]$ plots for all elements studied. Open squares represent non-host stars and filled squares represent host stars. Typical error bars are shown in the upper left of each panel. *Left Column:* O, Mg and Cr. *Center Column:* Y, Zr and Ba. *Right Column:* Eu and Nd.

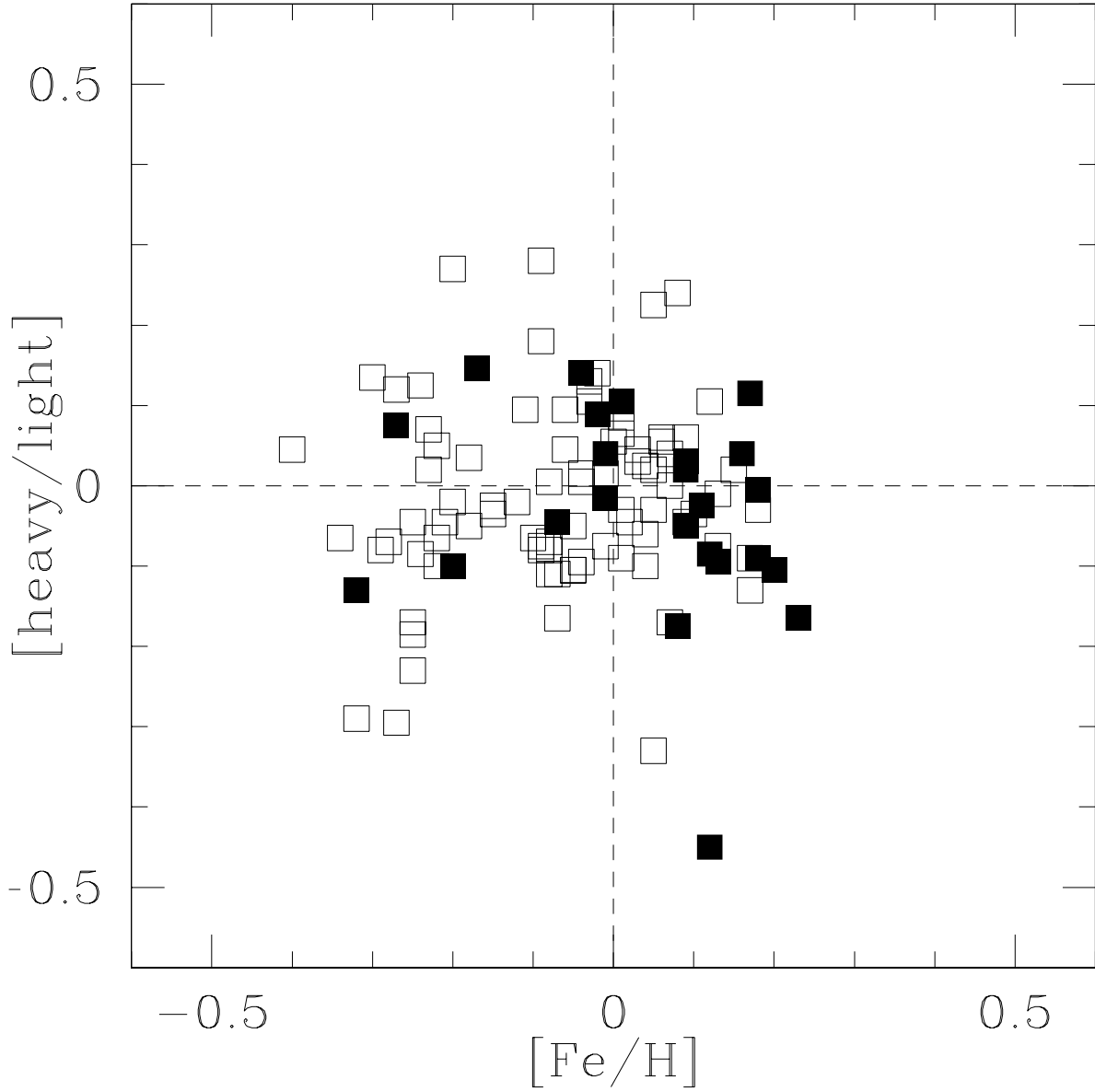


Fig. 3.— $[\text{heavy}/\text{light}]$ vs. $[\text{Fe}/\text{H}]$ plots for the five heavy elements examined as part of this study. For the definition of $[\text{heavy}/\text{light}]$, please see the text. Open squares indicate non-host stars, filled squares indicate host stars and dashed lines indicate solar values.

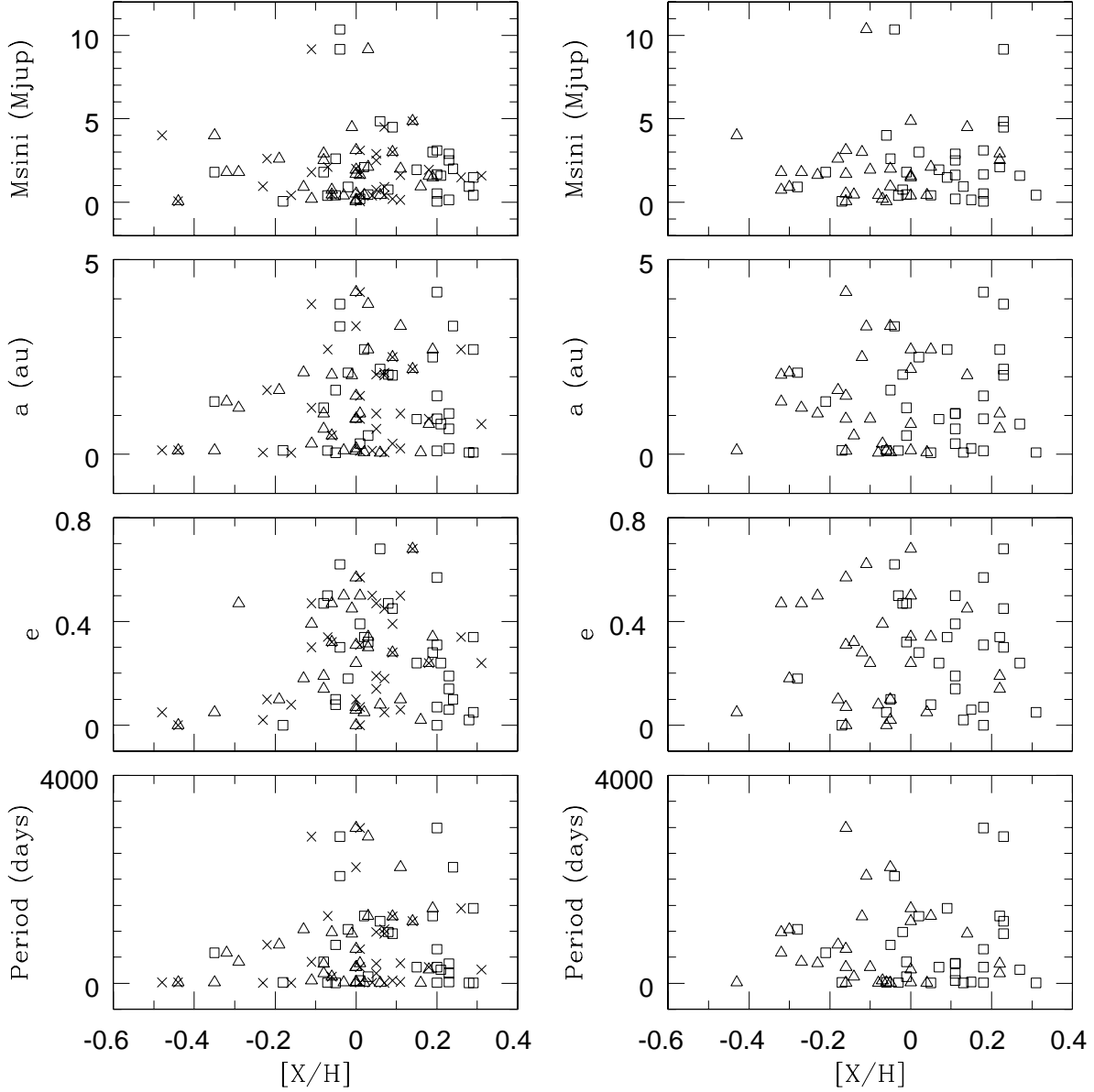


Fig. 4.— Orbital properties of extrasolar planetary systems vs. abundance of the heavy elements. HD164427 has been omitted. *Left:* s-process elements Y (triangles), Zr (squares) and Ba (crosses). *Right:* r- and mixed process elements Eu (triangles) and Nd (squares). *From top to bottom:* M_{sini} of the planet, orbital semi-major axis of the planet, eccentricity of the orbit of the planet and period of the planet.